ANL-78-63

ANL-78-63

DOMAIN AND SURFACE STRUCTURES OF SODIUM TUNGSTEN BRONZES, Na_xWO_3 ($0.4 < x < 1$)

by

Masao Atoji

U of C-AUA-USDOE

ARGONNE NATIONAL LABORATORY, ARGONNE, ILLINOIS

Prepared for the U. S. DEPARTMENT OF ENERGY
under Contract W-31-109-Eng-38

DISCLAIMER

Printed in the United States of America
Available from
National Technical Information Service
U. S. Department of Commerce
5285 Port Royal Road
Springfield, Virginia 22161
Price: Printed Copy $5.25; Microfiche $3.00

Distribution Category:
Chemistry (UC-4)

ANL-78-63

ARGONNE NATIONAL LABORATORY
9700 South Cass Avenue
Argonne, Illinois 60439

DOMAIN AND SURFACE STRUCTURES OF SODIUM TUNGSTEN BRONZES, Na_xWO_3 ($0.4 < x < 1$)

by

Masao Atoji

Chemistry Division

September 1978

THIS PAGE

WAS INTENTIONALLY

LEFT BLANK

TABLE OF CONTENTS

	Page
ABSTRACT	7
I. INTRODUCTION	8
A. General	8
B. Crystal Structure	10
C. Surface Properties	12
D. Applications	13
E. Definitions, Provisions, and Terminologies	14
II. CHEMICAL PROPERTIES AND ETCHING	16
III. SUBSTRATE	17
IV. SURFACE FILM	28
A. Characterization and Formation	28
B. Structural Aspects	33
C. Properties	37
D. Effect of Temperature	41
E. Effect of Pressure	48
V. ELECTRONIC SPECTROSCOPY, MICROSCOPY, AND DIFFRACTION	50
A. X-ray Photoelectron Spectroscopy	50
B. Electron Microscopy and Diffraction	51
ACKNOWLEDGMENTS	57
REFERENCES	58

LIST OF FIGURES

No.	Title	Page
1.	Unit Cell for Perovskite-type ABO_3 Compound	9
2.	A Slightly Distorted Perovskite Structure of $Na_{0.75}WO_3$	11
3.	Unpolarized-light Photomicrographs Showing Sodium Segregation on Mechanically Polished (010) Surfaces of $Na_{0.7}WO_3$ and $Na_{0.75}WO_3$	18
4.	Unpolarized-light Photomicrograph of Slightly Etched (010) Surface of $Na_{0.68}WO_3$, Showing Random Segregation of Sodium Atoms near Surface of Substrate.	20
5.	Unpolarized-light Photomicrograph of Slightly Etched (010) Surface of $Na_{0.75}WO_3$, Showing Sodium Segregation in a Venetian-blind Pattern.	21
6.	Nomarski Interference-contrast Photomicrograph of Etched (010) Surface of $Na_{0.75}WO_3$, Showing Pseudoperiodic Segregation of Sodium Atoms	22
7.	Nomarski Interference-contrast Photomicrograph of Deeply Etched (010) Surface of $Na_{0.7}WO_3$, Showing Parallel Subgrain Boundaries	23
8.	Nomarski Interference-contrast Photomicrographs of Deeply Etched (010) Surfaces of $Na_{0.75}WO_3$ Crystals	24
9.	Polarized-light Photomicrograph of an Electrolytically Synthesized Film Covering a Deeply Etched (010) Plane of $Na_{0.75}WO_3$	29
10.	Polarized-light Photomicrographs of Deeply Etched (010) Surface of $Na_{0.68}WO_3$ Covered with Surface Film.	30
11.	Polarized-light Photomicrograph at Maximum Birefringent Contrast of Electrolytically Synthesized Surface Films on Polished (010) Plane of $Na_{0.71}WO_3$	31
12.	Polarized-light Photomicrograph of Electrolytically Synthesized Surface Films on Polished (010) Plane of $Na_{0.75}WO_3$	32
13.	Nomarski Interference-contrast Photomicrograph of Etched (110) Surface of $Na_{0.75}WO_3$ Crystals.	34
14.	Nomarski Interference-contrast Photomicrograph of Etched (111) Surface of $Na_{0.75}WO_3$	35
15.	Polarized-light Photomicrographs of Matched Pair of Cleaved (010) Surfaces of $Na_{0.75}WO_3$	39

LIST OF FIGURES

No.	Title	Page
16.	Unpolarized-light Photomicrographs of Matched Pair of Cleaved Surfaces of $Na_{0.75}WO_3$	40
17.	Transition Temperatures of Pseudocubic Na_xWO_3, $0.35 < x < 1$	43
18.	Temperature Dependencies of Lattice Parameters and Crystal Structures of Four Structural Phases of $Na_{0.81}WO_3$	44
19.	Polarized-light Photomicrographs Showing Temperature Dependency of Domain Structure of Surface Film of $Na_{0.70}WO_3$ at 0-150°C	46
20.	Polarized-light Photomicrographs Showing Temperature Effect on Surface Film of $Na_{0.6}WO_3$ at 23-140°C	47
21.	Polarized-light Photomicrographs Showing Effect of External Pressure on Domain Structure of Surface Film of $Na_{0.75}WO_3$	49
22.	Unpolarized-light Photomicrograph of Argon-sputtered (010) Surface of $Na_{0.75}WO_3$	52
23.	Scanning-electron Micrograph of Deeply Etched (010) Surface of $Na_{0.75}WO_3$	53
24.	An Enlarged View of Fig. 23	54
25.	Electron-diffraction Pattern of (hk0) Zone of $Na_{0.75}WO_3$	55
26.	Electron-diffraction Pattern of (h 3k k) Zone of $Na_{0.75}WO_3$	56

TABLE

No.	Title	Page
I.	A Survey of Temperature-dependency Measurements on Various Physical Properties of the Sodium-Tungsten Bronzes	42

THIS PAGE

WAS INTENTIONALLY

LEFT BLANK

DOMAIN AND SURFACE STRUCTURES OF SODIUM TUNGSTEN BRONZES, Na_xWO_3 ($0.4 < x < 1$)

by

Masao Atoji

ABSTRACT

The domain and surface structures of metallic sodium tungsten bronzes, Na_xWO_3, $0.4 < x < 1$, have been studied using mostly optical microscopy, supplemented by chemical methods, photoelectron spectroscopy, electron microscopy, etc. The birefringent, multidomain structure of the bronze is exhibited by a sodium-deficient, epitaxial surface film and hence is not, as reported elsewhere, a bulk property. The film can be synthesized by anodic electrolysis in alkaline solution and can exist only epitaxially with the substrate. It is chemically inert, translucent, and often laminated to a multilayered film. The film domain is hypersensitive to lateral stress and to thermal change, and appears to be modulated by minute structural changes of the substrate. This epitaxial modulation of the film is strikingly large at the phase transitions of the substrate induced by slightly different tiltings of the oxygen octahedra. The domain-wall movement is often slow enough to be visible, and that by thermal effect is occasionally accompanied by an audible, high-pitched, snapping sound.

The substrate exhibits pseudoperiodic subboundaries that are probably caused by growth defects and by the segregation of the sodium atoms in the bulk structure. The sodium segregation occurs also on the surface of the substrate and tends to precipitate in a variety of periodic patterns. Electron-scanning microscopy revealed an interesting example of a compositional segregation accompanying a morphological segregation. These bulk and surface structures of the substrate are nonbirefringent and indicate neither optical nor morphological changes at the phase transitions. Argon-ion sputtering on the surface creates nonbirefringent, multistriped domains that are not mechanical twins but are alternating arrays of two different decomposed species.

I. INTRODUCTION

A. General

This work is part of our study on inorganic metals, which are defined as metallic substances consisting of metallic and nonmetallic elements. Exemplary inorganic metals are inorganic bronzes, metal carbides, metal nitrides, etc., many of which exhibit challenging physical, chemical, and technological properties. For example, in most inorganic metals, the conduction-wave function enhances the valency bonding, leading to a substantial increase in conductivity, melting point, and hardness. Typically, the electrical conductivity of ZrN is twice that of zirconium metal. Some rare-earth carbides are much better conductors than rare-earth metals. Carbides and nitrides of titanium, zirconium, and hafnium melt 1000-2000°C higher than the respective parent metals. TiC, ZrC, TaC, and WC exhibit very high hardness, which classifies them in the group second to diamonds. Some inorganic metals possess high superconduction transition temperatures, e.g., $Nb_{0.3}N_{0.7}$ (17.5 K), $Y_{1.4}Th_{0.6}C_3$ (17 K), NaCl-type MoC (12 K), and α-WC (10 K). The technological application is promising in electrochemical, catalytic, and related developments.

Similarly, the inorganic bronzes exhibit fascinating properties. The bronze comprises the metal-oxide lattice as the host matrix, the positive ions as the interstitial guests, and an equivalent number of conduction electrons. The oxides of high-valency metals such as tungsten, vanadium, molybdenum, tantalum, and titanium accommodate the guest ions such as alkalis, alkaline earths, rare earths, copper, silver, uranium, hydrogen, and ammonium. The inorganic bronzes have been reviewed by Hägg and Magnéli (1954), Sienko (1963), Shanks et al. (1963), Ribnick et al. (1963), Wadsley (1964), Dickens and Whittingham (1968), Galasso (1969), Hagenmuller (1971), Bevan and Hagenmuller (1975), and Gamble and Geballe (1976). Closely related subjects are metallic metal oxides, which have been reviewed by Goodenough (1971).

The most extensively studied inorganic bronzes are sodium tungsten bronzes, Na_xWO_3 with $0.45 < x < 1$, which are metallic and exhibit perovskite or its modified structure (see Figs. 1 and 2). The electronic formla of Na_xWO_3 may be written as $xNa^+ + WO_3 + xe^-$, where W is hexavalent and e^- is a quasi-free conduction electron (Kupka and Sienko, 1950; Gardner and Danielson, 1954; Greiner et al., 1962; Shanks et al., 1963; Sienko, 1963; and Zumsteg, 1976). The electronic energy levels and wave functions of the bronze have been discussed by Keller (1960), Vest et al. (1958), Jones et al. (1962), Mackintosh (1963), Giuliani et al. (1972), and Kopp et al. (1977). The lattice energy and the thermodynamic data have been studied by Smith (1954), Ramanarayanan and Worrell (1974), and Whittingham (1975).

The present report emphasizes that inhomogeneities in bulk and surface structures play important roles in the bronze study. Elaborate theories have been formulated for the bronze properties, but these theories are often based on experimental data that are erroneous because of the sample inhomogeneity.

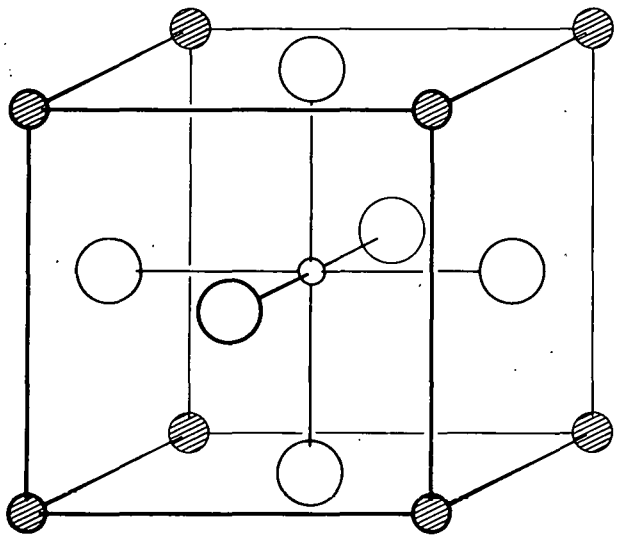

Fig. 1

Unit Cell for Perovskite-type ABO_3 Compound. ANL Neg. No. 122-78-632.

An instructive case in this aspect is the electrical-resistivity study of sodium tungsten bronzes carried out by G. C. Danielson's group. Their first resistivity measurement (Gardner and Danielson, 1954) indicated a minimum near $x = 0.75$ which was interpreted as a nearly complete ordering of the sodium atoms. Their second study (Ellerbeck et al., 1961) found that the resistivity minimum at $x = 0.75$ is caused by sample inhomogeneity and that homogeneous crystals showed no minimum and hence no sodium ordering. The third study (Muhlestein and Danielson, 1967b) found that highly homogeneous crystals exhibit a different, smaller anomaly near $x = 0.75$, meaning a partial sodium ordering.

The electronic transport properties of the bronzes were interpreted based on various clustering models regarding the sodium distribution: a linear-polymer-like clustering (Fuchs, 1965), a randomly linked clustering (Lightsey, 1973), and $NaWO_3$ globules surrounded by WO_3 (Fromhold and Narath, 1964; Roper and Knowles, 1972; Webman et al., 1976). However, these clustering models ascribing microscopic inhomogeneity have been rejected by Tunstall (1976), Crandall and Faughnan (1977), and Weinberger (1978). This perplexity is largely attributed to macroscopic inhomogeneity in the bronze specimen.

The optical reflectance spectra of sodium tungsten bronzes have been measured repeatedly to obtain congruous electronic energy values (Brown and Banks, 1954; Dickens et al., 1968; Lynch et al., 1973; Camagni and Manara, 1977a and 1977b). There are still vital inconsistencies among these measurements. Inhomogeneities in the surface structure should be largely responsible for this.

The X-ray photoelectron spectra of the bronzes indicated satellitic energy levels, which were explained in terms of a plasmon excitation (Campagna et al., 1975). This was rebuked by DeAngelis and Schiavello (1976), who interpreted the satellites by assuming the coexistence of W^{6+}, W^{5+}, and W^{4+}. The multivalency model was immediately discarded by Campagna's group (Wertheim et al., 1976), cautioning that the bronze surface and hence the satellitic spectra are very sensitive to oxygen and water in the environment. However, the refined spectra of Campagna's group (Chazalviel et al., 1977) are inconsistent with the plasmanon model and call for new concepts.

Šepa et al. (1967) first reported a strong electrocatalytic activity of the tungsten bronze in the cathodic reduction of oxygen (see also Sec. I.D below). Bockris and McHardy (1973) have shown that this catalytic activity exists only with the trace amount of platinum contaminant that was introduced during the electrolytic synthesis of the bronze crystal using the platinum electrodes. However, Randin (1974d and 1975) asserted that his bronze crystals showed no catalytic activity, despite the platinum contaminant. This topic indicates the intricacy of the surface property. Similarly complex problems persist in the bulk crystal structure as described in the following sections.

This report characterizes structural and compositional inhomogeneities by revealing a variety of twinnings, domains, and compositional segregations in the surface and bulk structures. The major finding is that the $BaTiO_3$-like multiple twin structure of the bronze is not a bulk property, but a surface phenomenon exhibited by an epitaxial film. A unique technique was also discovered for creating unprecedently well-crystallized twinned film. This process has facilitated an extensive exploration of domain properties such as remarkable pyro- and piezostrictive phenomena. Other physical and chemical properties of the film and the substrate are also presented. The surface and bulk properties reported here should be of considerable value in electrode, catalysis, and superconductivity applications (see Sec. I.D).

B. Crystal Structure

The sodium tungsten bronzes were first prepared by Wöhler (1824). The X-ray structure study of the bronze was initiated by de Jong (1932). He assigned the bronze structure to the ideal perovskite type on the basis of the cubic sublattice of tungsten and the assumed positions of oxygen and sodium (shown in Fig. 1). Until recently, the X-ray structure was refined only on the cubic unit-cell dimension a_0 at various x values (Hägg, 1935; Brown and Banks, 1954; Wechter et al., 1968). A representative result is a_0 (Å) = $0.0819x + 3.7846$ of Brown and Banks (1954).

By polarizing microscopy measurements, Ingold and DeVries (1958) discovered that the bronze single crystal exhibits birefringent, twin domains at room temperature. The optical characteristics were interpreted in terms of a tetragonal cell with c/a slightly less than one (between 0.990 and 1.000)

and twinning on {101}. They also found that the domain boundaries can be modulated by the bending stress and that the tetragonal phase transforms to the cubic structure on cooling and also on heating, e.g., at -13°C and 146°C for x = 0.75, respectively. Ingold and DeVries interpreted all these observations as the bulk properties.

Atoji and Rundle (1960) have reported the first neutron-diffraction study of the bronze. The results were as follows: The bronze structure is a distorted perovskite type at 296-77 K (as shown in Fig. 2); the X-ray unit-cell dimension has to be doubled; the sublattice symmetry is O_h-m3m for tungsten and sodium; it is T_d-$\bar{4}$3m or its twinned group for oxygen; the oxygen octahedra are tilted alternatively about 4° in the <110> directions; and the sodium atoms are not necessarily all equivalent and can be distributed in two different atomic sites.

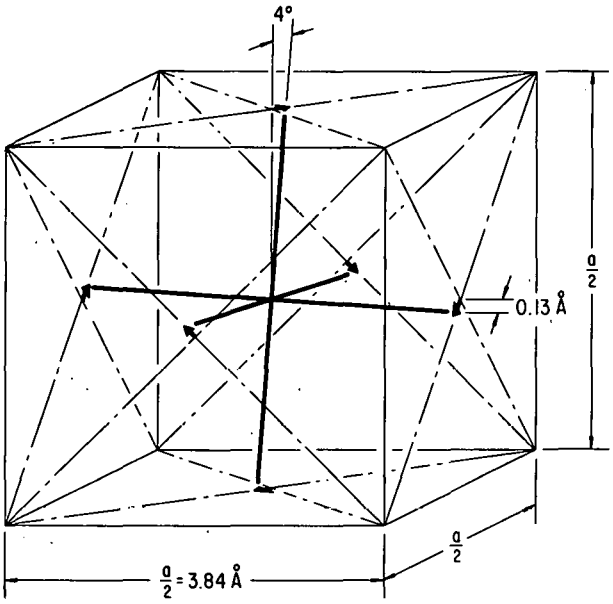

Fig. 2. A Slightly Distorted Perovskite Structue of $Na_{0.75}WO_3$. The small arrow indicates the direction and the magnitude of the displacement of the oxygen atoms in T_h^5-Im3 from the perovskite position O_h^1-Pm3m. The tilting angle is about 4° along <110>. The resulting displacement is 0.13 Å, which is comparable to the root-mean-square displacement of 0.1 Å in thermal vibration at room temperature. ANL Neg. No. 122-78-633.

The sodium assignment is largely based on space-group considerations. Various order-disorder distributions of the sodium atoms yield hardly different intensity values. Atoji and Rundle (1960) presented the most probable distribution of the sodium atoms, but did not elaborate on the intrinsically large uncertainty involved due to the space limitation of short communication. Notwithstanding, several authors have misinterpreted the sodium distribution of Atoji and Rundle (1960) as conclusive evidence of the ordering at x = 0.75.

The neutron reflections of Atoji and Rundle (1960) showed abnormal peak broadening in some zones, indicating a complex admixing of growth defects and certain twinnings. The peak profile analysis was difficult; hence overall integrated intensities were used to obtain an averaged structure.

A recent neutron study at room temperature (Wiseman and Dickens, 1976) was based solely on powder data. More recently, by means of single-crystal X-ray lattice-parameter measurements, Clarke (1977) found an additional transformation within the tetragonal region, leading to four known structure phases. They are designated here as Cubic I, Tetragonal I, Tetragonal II, and

Cubic II. The transition temperatures are successively, e.g., T_1 = -8, T_2 = 54, and T_3 = 147°C for x = 0.75 (see Sec. IV.D). The tetragonality c/a is in the range of 1 to 0.998, the median value being about 0.9987. The above symmetry assignments and the proposed structures of Clarke (1977) (see Sec. IV.D) have not been established unambiguously. A Raman scattering study (Flynn et al., 1978) also found these four phases using the samples obtained from the same batch as Clarke's (1977). These samples had been heated in air, but the resulting surface oxidation was assumed to be insignificant.

During the past 20 years, although intermittently, we have carried out many X-ray diffraction experiments at room temperature in order to detect the noncubic lattice distortion and the superlattice reflection. In the single-crystal study, we have used back-reflection-Laue, rotation-oscillation, and zero- and upper-level precession methods, all with exceedingly long exposure time. The reflection profiles were carefully studied to detect any abnormal features. Numerous powder-diffraction experiments have been similarly carried out. These X-ray experiments detected neither noncubic lattice distortion of $c/a > 0.9996$ nor superlattice reflection.

Wiseman and Dickens (1976) detected c/a = 0.9992 on their bronze samples but have nevertheless proceeded with the structure analysis based on cubic symmetry.

In conjunction with our neutron study, I have examined untreated and treated surfaces of numerous bronze samples using polarized-light microscopy. I confirmed most of the Ingold-DeVries (1958) observations, but found some inexplicable aspects. My subsequent experiments indicated that the Ingold-DeVries observations were most likely made on sodium-deficient, expitaxial surface films. The explanation of this conclusion is a major subject of this report.

C. Surface Properties

The surface-related properties of the bronzes have been reported in a number of publications. Spitzin and Kaschtanoff (1928) stated that the bronze powders (1-20 μm) contain adsorbed water to the extent of about 0.4 wt % (6 mol %), which can be driven off by heating at 200-300°C. Straumanis and Dravnieks (1949) observed that, when the sintered bronze is exposed to moist air, the electrical resistivity increases with time, probably owing to the formation of a surface layer at the intergrain boundaries.

A preliminary electron-diffraction work of Muldawer (1962) indicated that the surface of a $Na_{0.7}WO_3$ single crystal immersed in HF and/or exposed to moist air was converted partly to the tetragonal bronzes ($x \simeq 0.1$) and partly to tungsten oxides such as W_4O_{11} (tetragonal). Consadori and Stella (1970) observed that bronze exposed to air exhibits time-dependent optical-reflectivity spectra, indicative of a film growing on the surface.

Vojnovic et al. (1972) proposed a structure model of a hydrated layer of nonstoichiometric oxide, which is presumably formed electrochemically on the surface of the bronze electrode in acidic solution. This aspect was studied more quantitatively by McHardy and Bockris (1973) using optical-reflectance spectroscopy and ion-probe mass spectroscopy. They found that the bronze surface is partly depleted in sodium, typically from 0.7 to 0.25 in x, to a depth of about 500-2000 Å, and exhibits n-type semiconducting characteristics. Likewise, Šepa et al. (1974) have proposed that the bronze surface in contact with aqueous media hydrates spontaneously, followed by a depletion of sodium through the irreversible exchange with hydrogen ions. This process occurs more readily in alkaline solution. Similarly, Vondrak and Balej (1973 and 1975) have studied the hydrogenation process yielding a sodium-deficient, hydrated layer on the bronze surface.

Wertheim et al. (1976) have demonstrated that the X-ray photoelectron spectra of the vacuum-cleaved surface of the bronze crystal change considerably by mere 10 min exposure to air. Preliminary work on the Auger spectrum and low-energy electron diffraction (Langell and Bernasek, 1977) revealed some unexplainable features of the bronze surface.

Unfortunately, none of these surface-related studies carried out the polarized-light microscopic observations.

For introductive reviews on physical and chemical techniques for surface study, see Kane and Larrabee (1974). Oxide and oxide films of metal have been reviewed by Diggle (1972 and 1973).

D. Applications

Technological applications of the bronzes appear very promising. The bronze possesses high electrical conductivity (comparable to graphite) and is very inert in acid media. Hence, the bronze can be an economical substitute for noble metals, particularly as electrode materials in acidic environments. Extensive studies have hence been pursued on the bronze electrodes in a wide range of electrochemical systems. Typical applications are indicating electrodes in analytical and synthetic reactions for acid-base, oxidation-reduction, metal-complexing, metal-chelating, etc. (Šepa et al., 1967, 1972, and 1974; Vojnovic and Šepa, 1969; Vojnovic et al., 1972; Wechter et al., 1972 and 1973; Vondrak and Balej, 1973 and 1975; Randin et al., 1973; Randin, 1973, 1974a, and 1974c; Randin and Vijh, 1975; Amjad and Pletcher, 1975; Dickens, 1977). In a recent application, the bronze and the reference electrodes in water generate an electric potential which is a sensitive function of the dissolved oxygen; this assembly can be conveniently used for monitoring the oxygen level in water-pollution control (Hahn et al., 1973).

The bronzes are also invaluable in catalysis and related applications. The bronzes can catalyze the ortho-para conversion of hydrogen and the

hydrogen-deuterium exchange reaction in the gas phase (Jones, 1960). The bronze doped with platinum is as effective an electrocatalyst as the best known catalyst, platinum, in the electrochemical reduction of oxygen to water in acidic media (Šepa et al., 1967; Fishman et al., 1969; McHardy and Bockris, 1973; Bockris and McHardy, 1973; Moody and Taylor, 1973; Appleby and van Drunen, 1976). However, some platinum-doped bronzes showed weak activity (Randin, 1974d and 1975; Weber and Shanks, 1976). The bronze electrode catalyzes evolution and dissolution of hydrogen in acid solution (Bockris et al., 1968; Šepa et al., 1972). The bronze containing a trace of platinum enhances the catalytic oxidation of hydrogen, hydrocarbons, carbon monoxide, and reformer gas in fuel cells (Broyde, 1968; Niedrach and Zeliger, 1969; Armstrong et al., 1971). The surface characteristics play a vital role in these catalytic reactions and have been discussed often in these publications. However, none of these studies examined the bronze surface by polarized-light microscopy.

Other potentially useful properties and exploratory subjects for development applications are as follows: A bronze that is oxidized electrolytically in a mixed solution of lead nitrate and nitric acid can be used as a rectifier that is operable at temperatures as high as 200°C (Kopelman, 1956). Superconductivity has been found in Na_xWO_3 with $0.2 < x < 0.4$, where the obviously important role of the surface layer is yet to be explored (Shanks, 1974; Ngai and Silberglitt, 1976). A thin-film electrochromic display has been developed based on the electrochemically reversible reaction, $WO_3 + xNa^+ + xe^- \rightleftarrows Na_xWO_3$ (Green et al., 1976). The surface film of the bronze is also chemically inert, and its role in catalysis should be studied more extensively.

E. Definitions, Provisions, and Terminologies

The metallographic microscope used was the Carl Zeiss Ultrapot II with attachments for polarized-light and Nomarski interference-contrast techniques. Also used was an E. Leitz Ortholux microscope with a polarized-light attachment. All observations were made using reflected light in a bright field with a 10X eyepiece and a set of low-power objectives to minimize refractive convergency. The polarized-light photomicrographs were taken with slightly uncrossed (about 2°) Nicols. The scattering of polarized light in the reflecting specimen accompanies various modulations of the plane of polarization. This modulation is assumed to be linear or circular, but not elliptic.

Regarding the optical procedure and interpretation, see Ingold and DeVries (1958) for specific discussions related to the bronzes. For general treaties, see Gifkins (1970), Phillips (1971), Chadwick (1972), and McCall and Mueller (1973).

The bronze samples used in this study were the single crystals grown by the cathodic electrolytic reduction of a molten mixture of Na_2WO_4 and WO_3 (Shanks, 1972; Whittingham and Huggins, 1972; Weller and Grandits, 1972; DeMattel et al. 1976). The colors of the bronzes are purple, brick-red, orange,

and yellow at approximately x = 0.5, 0.6, 0.7 and 0.8, respectively (Dickens and Whittingham, 1968). Concerning terminologies, the reduced unit cell is meant to indicate the perovskite-based structure containing one Na_xWO_3. The surface film or simply the film is an abbreviation for the sodium-deficient, epitaxial surface film.

The twinned domain configuration is specified as follows: For example, the [001]·[010]·[100] domain denotes that the a, b, and c axes of the domain are parallel to [001], [010], and [100] of the reference coordinates as designated by the bulk crystal. The notation [001]·[010]·[100]:(011):[001]·[100] [010] represents a twinned system consisting of the [001]·[010]·[100] and [001]·[100]·[010] domains with the twin plane of (011) of the domain structure. For brevity, we may omit (011) in the above notation. Similarly, in a uniaxial domain structure, we can define the domain orientation by the direction of its optic axis (the c axis). For example, the [100] domain has its c axis aligned parallel to [100] of the bulk crystal. The twin notation given above then becomes [100]:(011):[010], or a simpler form of [100]:[010].

The symbols, pa and pe, abbreviating parallel and perpendicular, respectively, indicate the relationship between the c axis of the domain and a specific plane of the bulk crystal. For example, the c axis of the pa domain is parallel to the plane of the bulk crystal under observation. The pa-pa twins comprise two different pa domains, and the pa-pe twins consist of pa and pe domains. In lieu of pa and pe, a and c are used elsewhere (Jona and Shirane, 1962). For example, when the (010) plane of the bulk crystal is under examination, the pa-pa twins consist of the [100] and [001] domains, while the pa-pe twins comprise the [100] and [010] or the [010] and [001] domains. A similar convention used is, for example, the [110] stripes, meaning the stripes running parallel to the [110] axes.

As stated in Sec. I.B, the crystal symmetries and structures of four different phases proposed by Clarke (1977) have not been confirmed unambiguously. Nevertheless, Clarke's data are most comprehensive regarding the phase transitions and hence are often taken as standards for descriptive convenience.

The optical anisotropy of the film can be described as being due to a tetragonal symmetry. We choose the [001] axis as an optic axis. In a given twinned structure, the direction of the [100] domain may coincide with the direction of [001] of another domain. Likewise, the [100] axis of a domain may become the [001] axis after a phase transition. Therefore, when the reference coordinates cannot be uniquely specified, we conveniently designate the {010} plane of the substrate as (010) and select [100] and [001] accordingly.

II. CHEMICAL PROPERTIES AND ETCHING

Since no specific chemical etchant for the bronze is given in the literature, many reagents were tested; the effects of each were examined by means of optical microscopy. In some cases, the sample was weighed before and after etching to estimate the rate of the reaction.

Straumanis (1949) stated that the high-x bronzes are decomposed to Na_2WO_4 by strong alkaline solution in the presence of oxidizing agents. He continued that the rate of the decomposition is slow with NaOH solution in the presence of oxygen, but fast with Na_2O_2. We found that all these reactions are exceedingly slow (less than 0.05% in weight loss per hour) and sometimes produce a surface film, in accordance with Šepa et al. (1974).

Straumanis (1949) also reported that the high-x bronzes are decomposed rather quickly by a mixture of nitric and hydrofluoric acids. Our test showed that this process is slow, the weight loss being about 0.5-2% per hour initially and much less subsequently. The reaction leaves a dark green deposit (probably WO_3) on the yellow bronze and a gray-tinted metallic-lustre film (probably tungsten oxides and tungsten metal) on the red bronze. These reaction products can be removed by hot NaOH solution, and this process produces certain film on the surface. To recapitulate, all these decomposition reactions are unsuitable for etching.

According to Brunner (see Magnéli, 1949a), the bronzes are readily decomposed by a concentrated solution of ammonium peroxy-disulfate $(NH_4)_2S_2O_8$. On the contrary, this reaction with or without the oxidizing catalyst $AgNO_3$ was found to be exceedingly slow (less than 0.1% weight loss per hour). Likewise, the fused $(NH_4)_2S_2O_8$ did not erode the bronzes. These processes are thus also inappropriate for the etching procedure.

The bronze is quite inert to acids. However, the inertness may be due to an exceedingly slow rate of reaction, which nevertheless may still be usable for etching. Accordingly, the bronze specimens were treated with commonly used etchants consisting of various acids (sulfuric, nitric, hydrofluoric, hydrochloric, perchloric, phosphoric, chromic, acetic, citric, picric, oxalic, etc.) (Kehl, 1949; Tegart, 1959). Similar trials were performed with typical bases (NaOH, KOH, NH_4OH, etc.). The bronze surface was not etched suitably by any of these reagents. In all cases, the weight loss was less than 0.1% per hour. Ingold and DeVries (1958) stated that they employed an etch-polishing method using HCl solution and 0.3 μm Al_2O_3 for revealing the domain structure. The bronze is inert to HCl; hence this process is actually just a mechanical polishing with the Al_2O_3 powder.

The bronze can be dissolved by an alkaline solution of potassium ferricyanide, $K_3Fe(CN)_6$ (Phillip and Schwebel, 1879; van Duyn, 1942). This reagent was found to be the only suitable etchant for the bronze. A solution

of 10% KOH and 10% $K_3Fe(CN)_6$, known as Murakami's reagent, is used for etching tungsten metal and carbide and other metal carbides and nitrides (Kehl, 1949; Tegart, 1959). For the bronze, we use oxygen-free solutions of 10-20% KOH or NaOH and 10-20% $K_3Fe(CN)_6$, which are termed modified Murakami reagents. The oxygen in the solution is readily removed by evacuating a flask container via rubber tubing (to permit manual agitation) in a mechanical-pump vacuum line. The etching was always performed while stirring the etchant vigorously and shaking the specimen very rapidly to attain a uniform reaction (Tegart, 1959). The presence of oxygen induces the formation of the surface film on the etched surface. The rate of the etching reaction with the modified Murakami reagent is faster for higher x.

III. SUBSTRATE

During the preparation of the metallographic specimen, some regions of the mechanically polished surface of the high-x bronze ($x > 0.7$, orange to yellow color) are tinted with brick-red color. The tinted area (darker in black-white photograph) varies from quite irregular to remarkably regular in shape (see Fig. 3). The reddish tinting implies a partial depletion of sodium that has taken place during the mechanical polishing. The X-ray microprobe analysis indicated that the sodium content in the red-tinted area is about 5 at. % less than that in the orange-yellow area. The color contrast is most effectively observed with unpolarized light and can be seen with or without the surface film. The color change is less noticeable in the lower-x bronzes.

The type and the degree of ordering in the segregation of the sodium atoms are to some extent dependent on the polishing procedure. The lesser strain (induced by polishing) appears to result in higher ordering in the segregation. A vibratory polishing, causing probably the least strain, yields the most regular pattern. Metallographic polishing by mechanical methods has been reviewed by Samuels (1971) and by McCall and Mueller (1973). Typical forms of the segregation are linear, rectangular, and crosshatched striations as shown in Figs. 3A, 3B, and 3C, respectively. The directions of these striations are always parallel to the $\langle 100 \rangle$ axes. The crosshatched or rice-field pattern as shown in Fig. 3C can also be produced on the polished {100} surface by anodic electrolysis in H_2O_2.

As described above, a given surface exhibits different types of the sodium segregation, depending on the surface treatment. Moreover, the sodium segregation of the surface is entirely different from the etch pattern of the same surface. Hence, the sodium segregation mentioned above probably occurs on the outermost layer of the unetched flat surface and is unrelated to the mechanical twinning. The diffusive migration of the sodium atoms is unlikely to occur in the bulk structure (Smith and Danielson, 1954), but may take place quite readily on the surface.

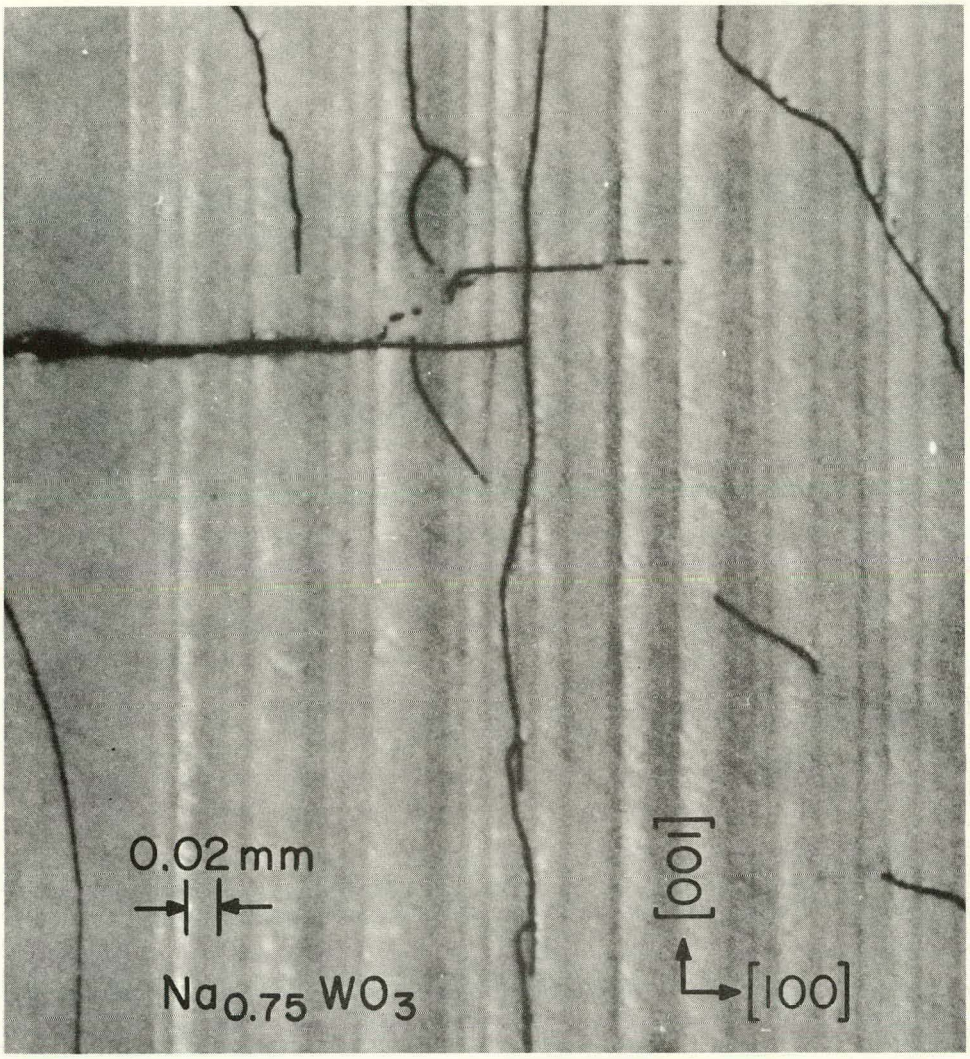

A

Fig. 3. Unpolarized-light Photomicrographs Showing Sodium Segregation on Mechanically Polished (010) Surfaces of $Na_{0.7}WO_3$ and $Na_{0.75}WO_3$. Linear, rectangular and crosshatched segregations of the sodium atoms are shown in A, B, and C, respectively. Dark and light regions represent reddish and orange colors, respectively. The sodium content in the former is about 5 at. % less than that in the latter. Weak optical birefringence, probably due to lattice strains, is observed along part of the narrow light band adjacent to the dark striation. The polishing was carried out using 0.25-μm diamond paste or water slurry of 0.3-0.5-μm Al_2O_3 powder. Samples A and B were polished using a uniform polishing technique; sample C was polished using an automatic vibratory-polishing machine. ANL Neg. Nos. (A) 306-78-10A, (B) 122-78-31A, and (C) 122-78-153 Rev.

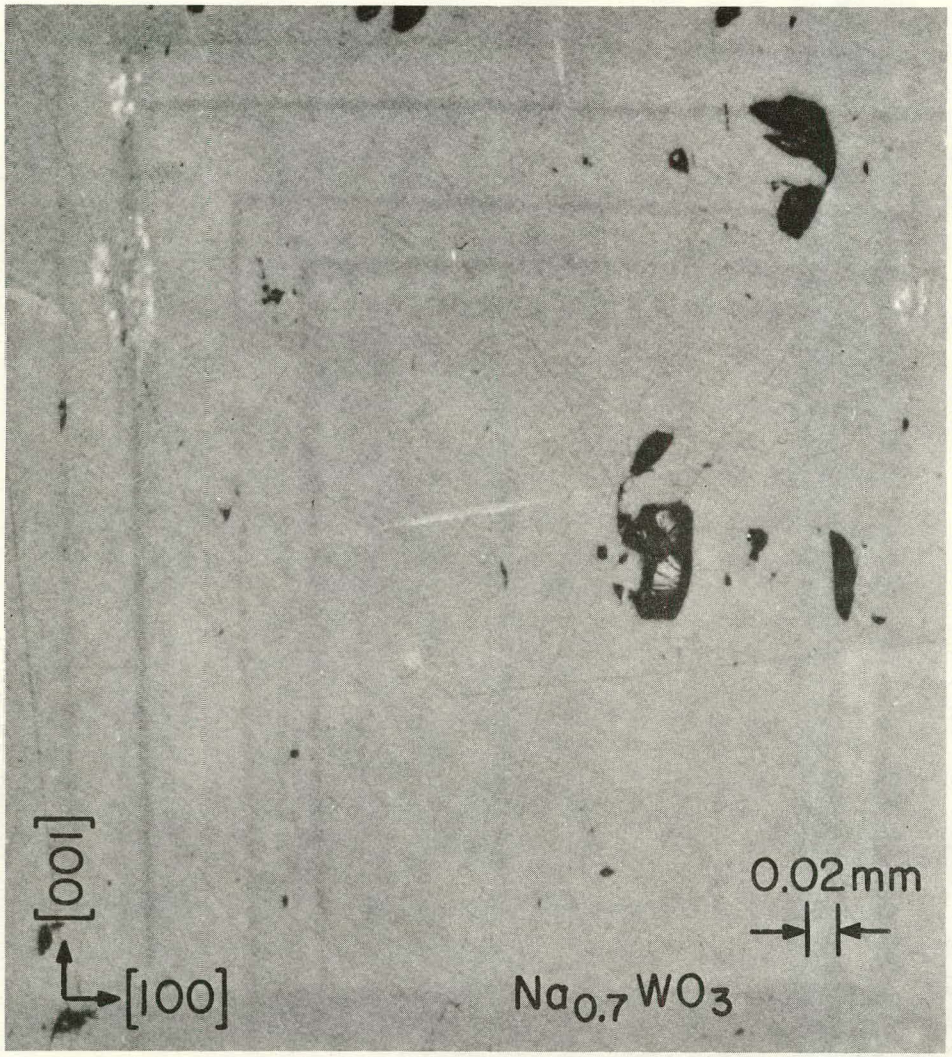

B

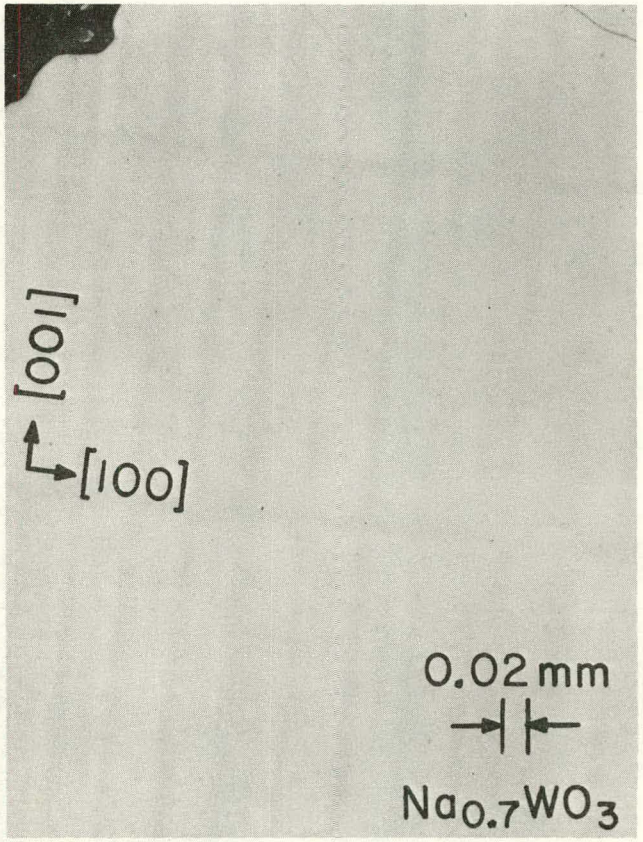

C

Fig. 3 (Contd.)

The sodium segregation is seen preferentially in the vicinity of surface blemishes such as pits, crevices, and cracks. Conversely, these macrodefects tend to occur along the segregation boundaries.

When the polished surface was etched slightly using the modified Murakami reagent, the treated surface showed a variety of etch patterns. Examples of the random and regular patterns are shown in Figs. 4 and 5, respectively. These observations imply that the sodium atoms near the surface also tend to segregate, frequently in striations parallel to the ⟨100⟩ axes.

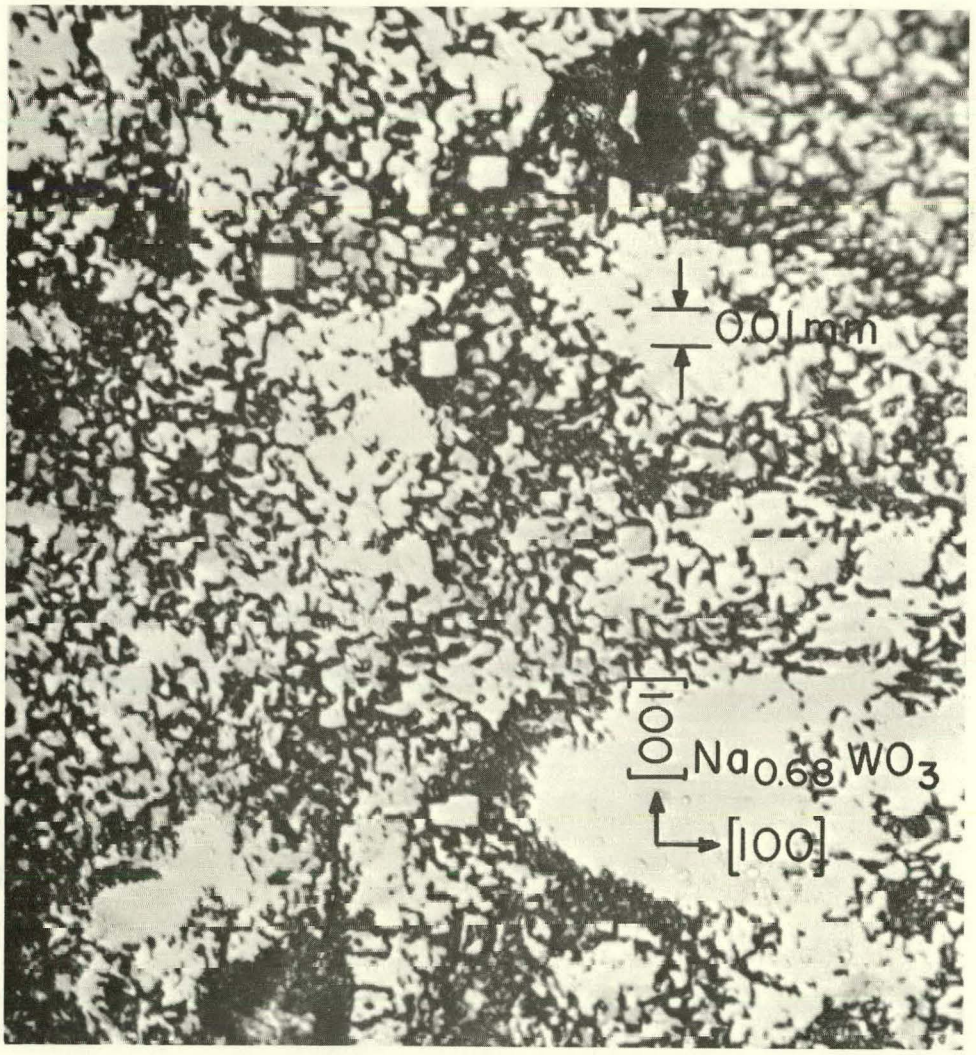

Fig. 4. Unpolarized-light Photomicrograph of Slightly Etched (010) Surface of $Na_{0.68}WO_3$, Showing Random Segregation of Sodium Atoms near Surface of Substrate. The surface was polished mechanically and then etched by a solution of 10% $K_3Fe(CN)_6$ and 10% NaOH at room temperature for a few seconds. The light areas were unetched, and the dark areas were etched out slightly. The sodium content of the dark area is higher than that of the light area. No optical birefringence was observed. ANL Neg. No. 122-78-392.

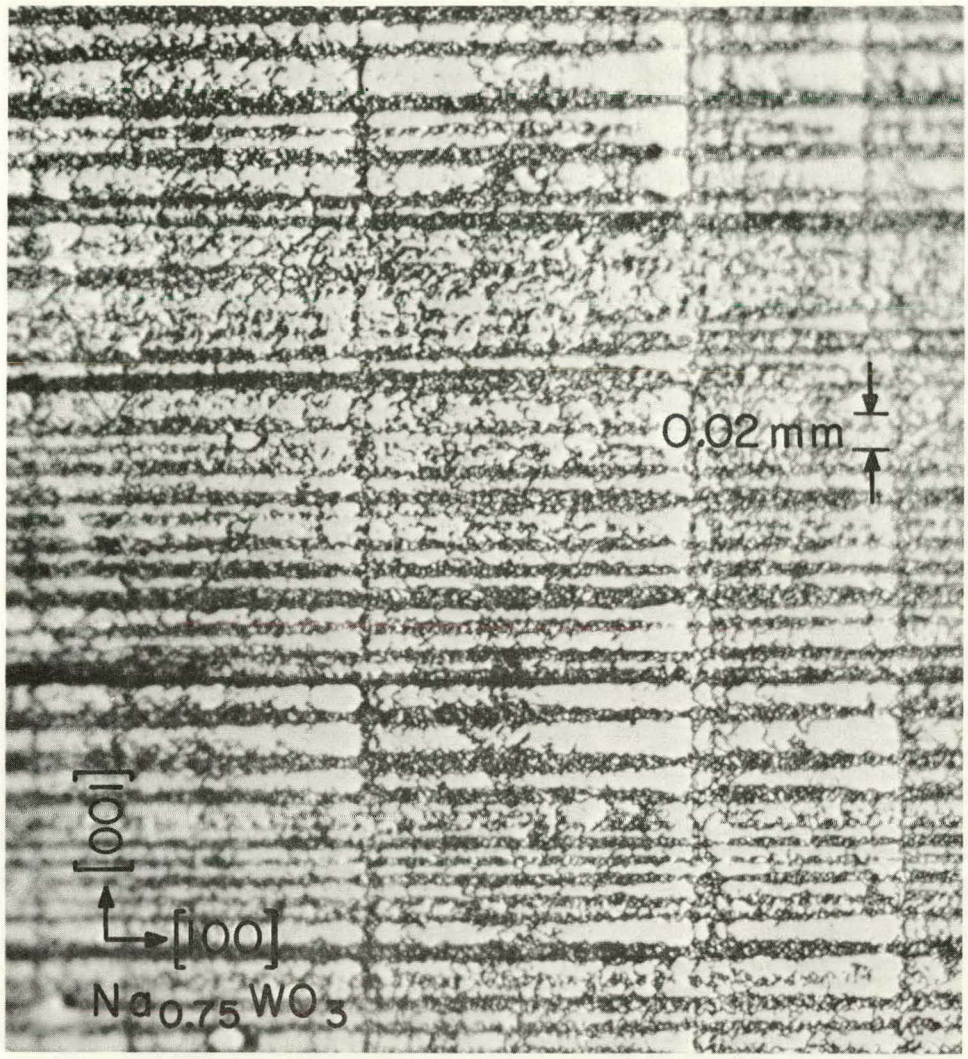

Fig. 5. Unpolarized-light Photomicrograph of Slightly Etched (010) Surface of $Na_{0.75}WO_3$, Showing Sodium Segregation in a Venetian-blind Pattern. The sodium content is higher in the darker area. The striations are parallel to the ⟨100⟩ axes. This surface showed no optical birefringence. The surface was mechanically polished and then etched using the modified Murakami reagent at room temperature. ANL Neg. No. 122-78-393.

The surface representing the bulk structure can be obtained by etching the surface deeply or by cleaving or crushing the crystal in vacuum. The deeply etched surface exhibits repetitive subboundaries, some of which show pseudodomain appearance (Figs. 6 and 7). The subboundaries are usually parallel to the ⟨100⟩ axes. Such pseudodomain modulations could be induced during the crystal growth.

The crystal growth by electrolytic reduction of molten mixtures of Na_2WO_4 and WO_3 undergoes several transient reactions at the solid-liquid interface (Brimm et al., 1951; Banks et al., 1970; Fredlein and Damjanovic, 1972; Whittingham and Huggins, 1972; Randin, 1974b). The crystallization is

regulated through the intercorrelation among supersaturation, nucleation, and diffusion, each of which has different temperature and potential dependencies. Under certain conditions, an integrated effect of these processes may generate a sinusoidal perturbation to the crystal growth, resulting in the pseudodomain morphology and the periodic segregation of the sodium atoms. A periodic perturbation arises when the nucleation takes place faster than the diffusion of the solutes in achieving critical supersaturation.

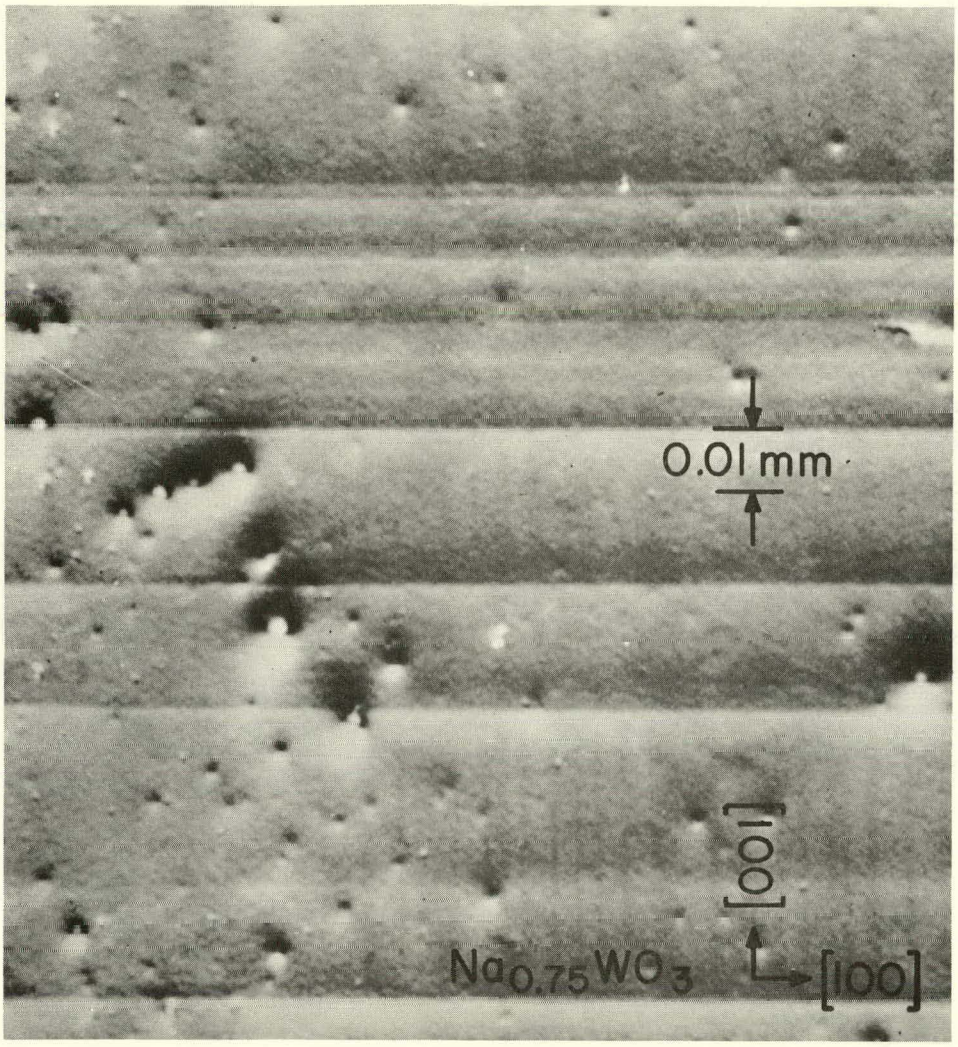

Fig. 6. Nomarski Interference-contrast Photomicrograph of Etched (010) Surface of $Na_{0.75}WO_3$, Showing Pseudoperiodic Segregation of Sodium Atoms. The parallel subboundary lines are slightly protruded. The diffusely bright bands adjacent to the striations show weak birefringence, which is probably induced by lattice strains. The etch pits could be end-on images of dislocations. Etching was performed using the modified Murakami reagent at room temperature for about 10 s. ANL Neg. No. 306-78-4A.

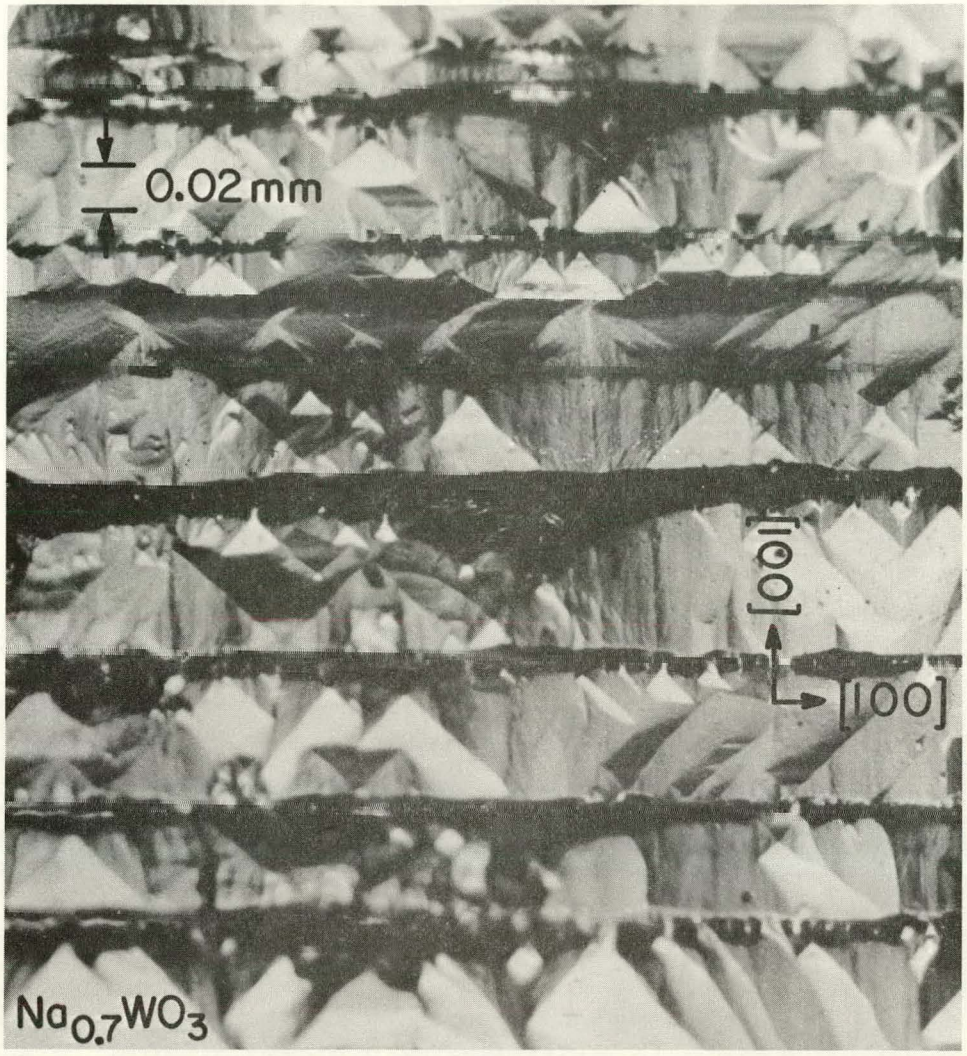

Fig. 7. Nomarski Interference-contrast Photomicrograph of Deeply Etched (010) Surface of $Na_{0.7}WO_3$, Showing Parallel Subgrain Boundaries. No optical birefringence was observed. The etching was performed using a boiling solution of 10% KOH and 10% $K_3Fe(CN)_6$ for about 10 s. ANL Neg. No. 122-78-444.

A similar effect can be produced by the commonly used automatic temperature controller with variable time constants, which gives rise to a small, periodic temperature fluctuation. If the temperature during growth is varied in steps, a periodic precipitation of impurities can occur in sectors. The impurity tends to precipitate preferentially on the {100} planes, creating readily cleavable planes (see Sec. IV.C).

The deeply etched substrates are shown in Fig. 8. These substrates are quite homogeneous in the sodium concentration. The etched figures on the {100} planes are characterized by the square pyramid having either O_h-m3m or T_h-m3 symmetry. The T_h symmetry is not necessarily intrinsic and may be attributed to the growth anisotropy. We have never observed the

morphological symmetries, T_d-43m, O-43, or T-23. This is also the case in the {100} and {111} studies (see Sec. IV.A). The substrate surface was also examined by Taylor (1969) from a different point of view.

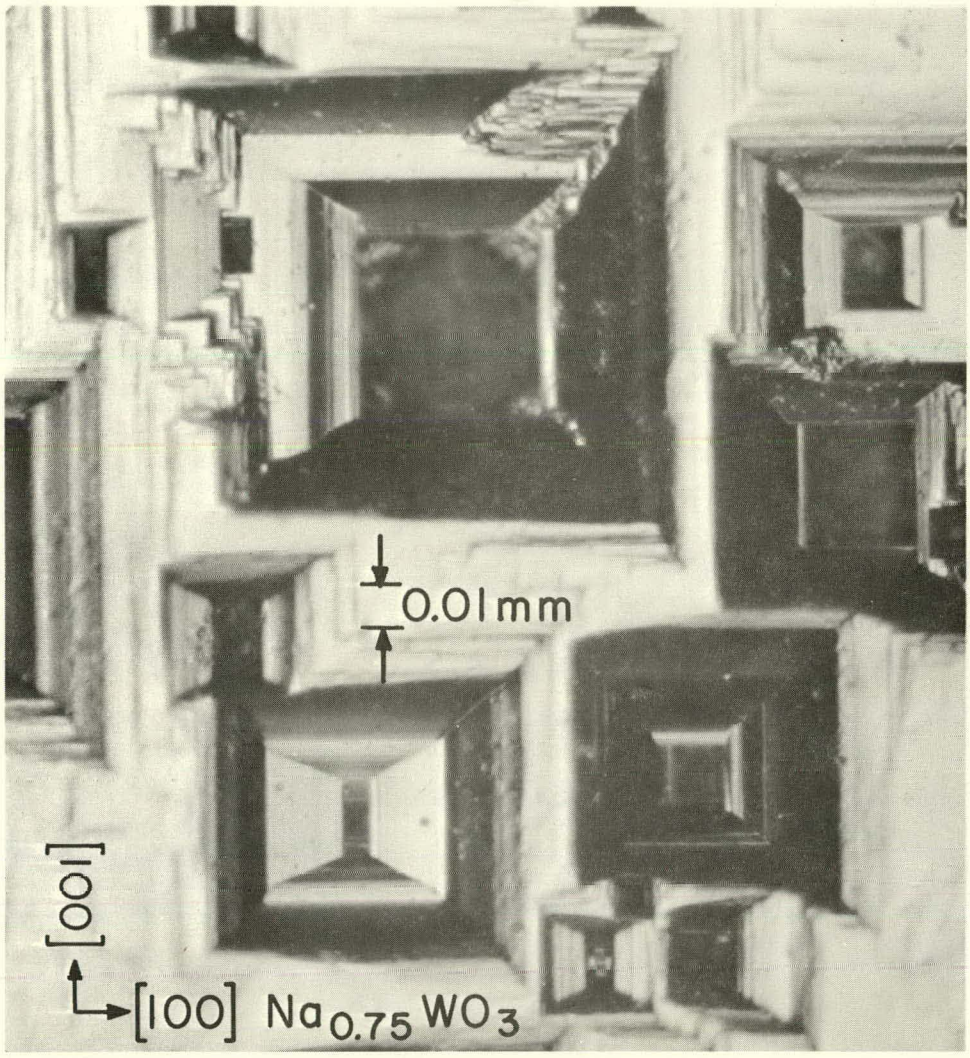

A

Fig. 8. Nomarski Interference-contrast Photomicrographs of Deeply Etched (010) Surfaces of $Na_{0.75}WO_3$ Crystals. The etched figures show morphological symmetries, O_h-m3m and T_h-m3. In Fig. 8B, some pyramid-figures have stepping striations which are always parallel to ⟨100⟩. A square diamond-shaped shadow, seen on the apex of the pyramid (one in Fig. 8B and many in Fig. 8C), is analyzed by scanning-electron microscopy in Figs. 23 and 24 (later). No optical birefringence was exhibited by these patterns. Etching was carried out using a boiling solution of 20% $K_3Fe(CN)_6$ and 20% NaOH for about 10 s. ANL Neg. Nos. (A) 122-77-945A, (B) 122-77-946A, and (C) 122-77-933A.

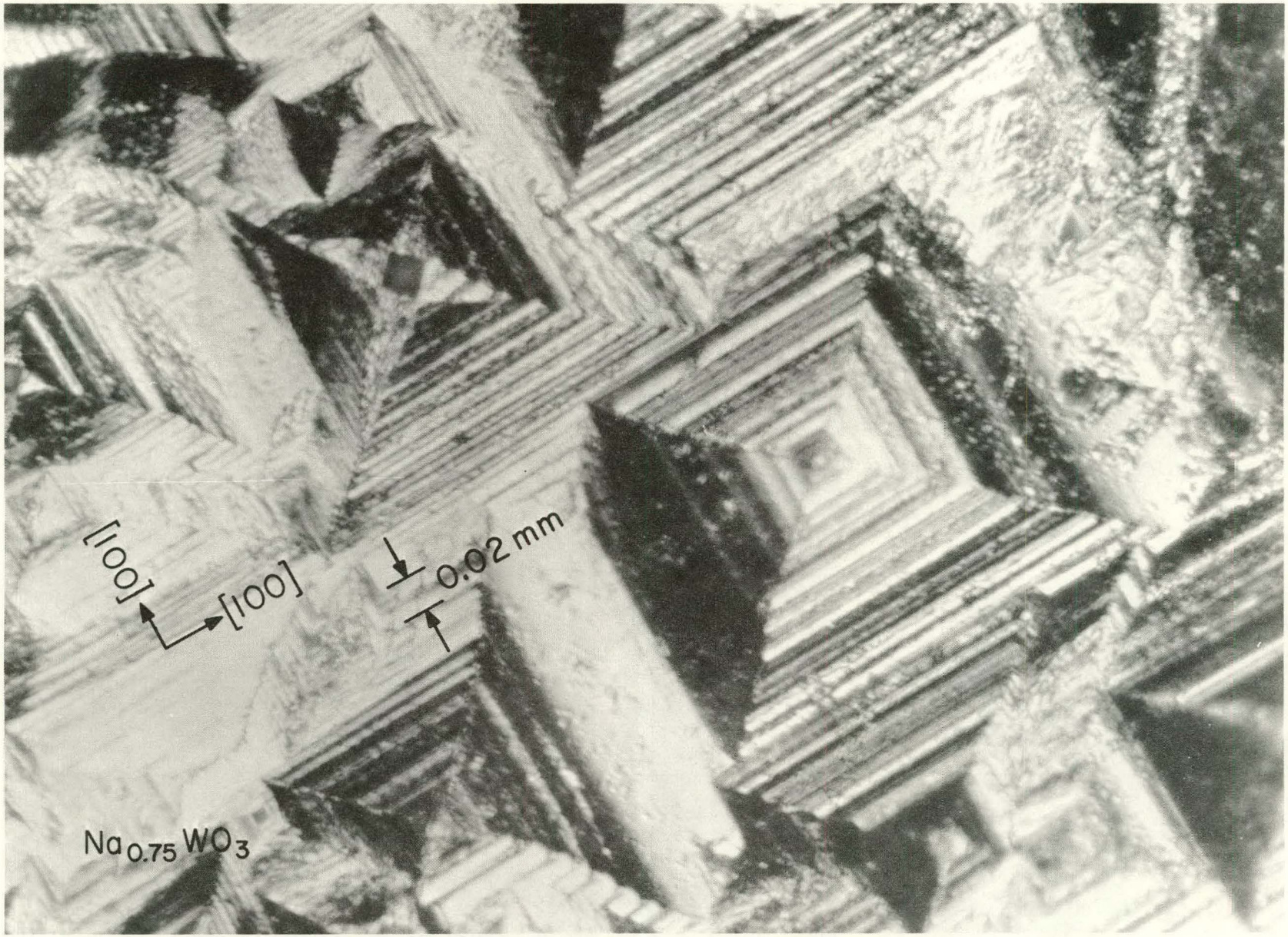

B

Fig. 8 (Contd.)

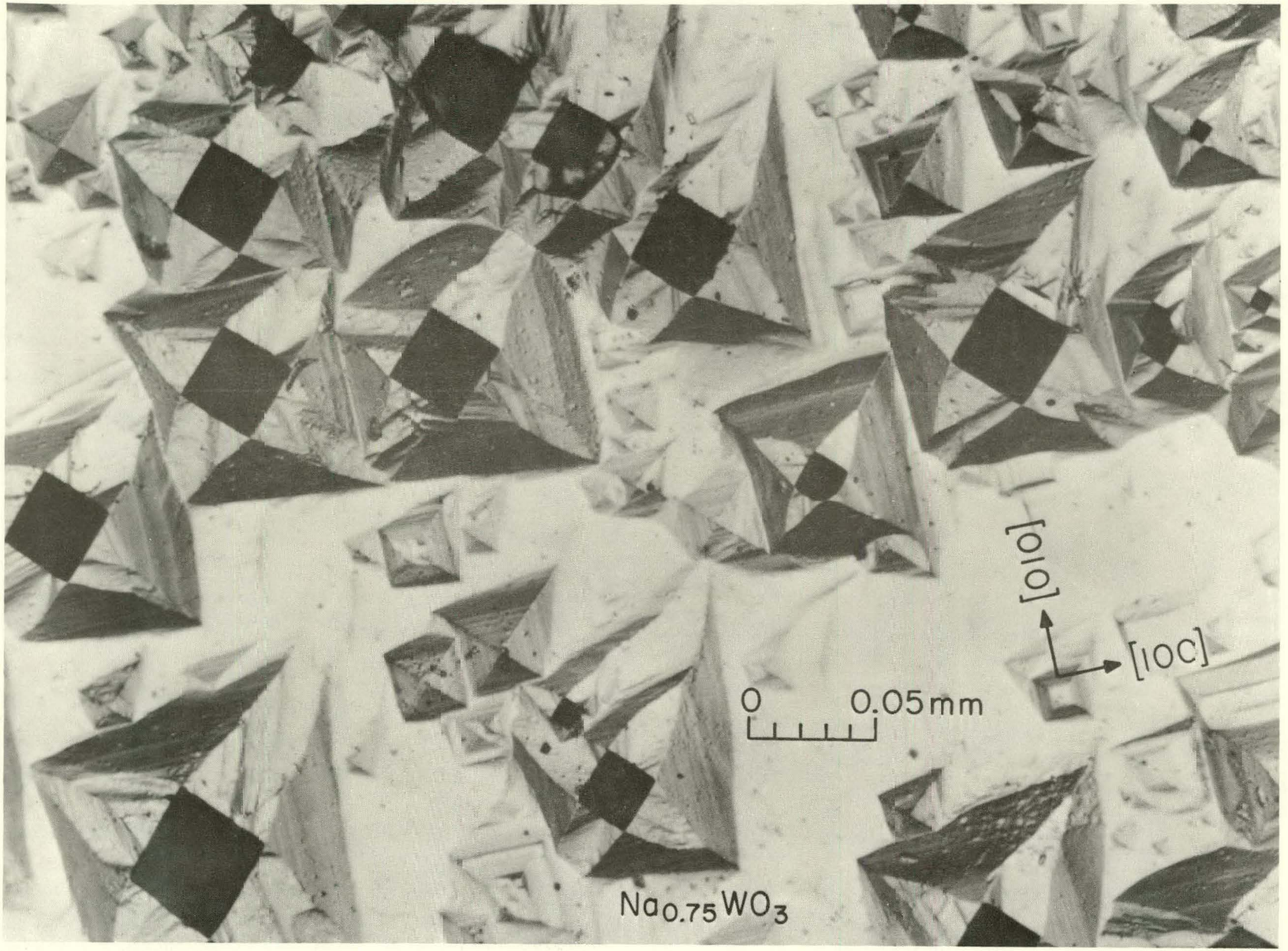

C

Fig. 8 (Contd.)

Regarding the optical birefringence of the substrate, weak optical extinctions were observed in some portions of a narrow line adjacent to the striation line (see Fig. 3). The optic axis is parallel to the reddish striation, and the optical extinction varies from vague to somewhat distinct. The extinction axis lies 45° from the [100] axis. Some striations are nonbirefringent, but become birefringent after being treated by NHO_3 and/or HCl. The birefringence is probably due to the local lattice strain caused by the sodium segregation.

Besides the above strain-induced effect, the surface, the near surface, and the deeply etched surface of the substrate show no significant birefringence and no change in optical and morphological properties at the phase transitions reported by Clarke (1977). Similarly, external stress on the substrate induced no measurable effect.

IV. SURFACE FILM

A. Characterization and Formation

We have observed the birefringent twin structure of the Ingold-DeVries type (1958) on some bronze single crystals and have verified most of their optical and related observations. However, there were some very puzzling aspects which could only be resolved by assuming that the Ingold-DeVries observations were specifically due to certain surface films.

First, the twinned surface layer is translucent to varying extents as evidenced below (see Figs. 9-12). The twin domain is unperturbed by minor surface blemishes (scratches, pits, and the like) which are visible through the twinned surface layer at both maximum and minimum contrasts in the birefringence. Also, it was observed, by virtue of translucency, that the blemishes are situated at a deeper focal plane. The differential focal depth indicated that a film thickness is about 10^{-2}-10^{-3} mm, or too thin to be measurable by an optical microscope. Simultaneously, the surface film was found to be single- or multilayered.

Second, using naturally occurring and artificially formed rectangular {100} prism crystals, we have tried to find any rational, coherent correlation among the twins of the orthogonal {100} faces. The Ingold-DeVries bulk-structure model should show, for example, the pa-pa twin on (010) and the pa-pe twin on both (100) and (001). So far, our effort at finding such a twin relation has been fruitless. This is also true for the synthetic film described below.

Third, and perhaps most important, we found that the twins of the Ingold-DeVries type can be synthesized on the untwinned surface by electrolytic anodization in alkaline solution. Typically, the bronze anode and the noble-metal cathode are placed in 10% NaOH or KOH aqueous solution. The electrolysis is performed at about 0.1-0.2 A/cm^2, 3-9 V dc for several seconds while stirring the electrolytic solution vigorously. In certain cases, the KOH solution gave a better result. A crystal, which is too small to be held by a clip, is placed in a platinum boat. A similar, but poor, yielding process is to wet the bronze surface with an alkaline solution in the presence of oxygen (see Sec. II).

The twinned films synthesized electrolytically over the etched surface are shown in Figs. 9 and 10, which demonstrate the enwrapping appearance of the surface film. The best twins can be created electrolytically on the polished {100} surface (see Figs. 11 and 12). The electrolytic synthesis suggests that the Ingold-DeVries twins are exhibited by a hydrated, sodium-deficient surface film (Šepa et al., 1974). This interpretation is supported by X-ray photoelectron and Auger Spectroscopic measurements (see Sec. V.A).

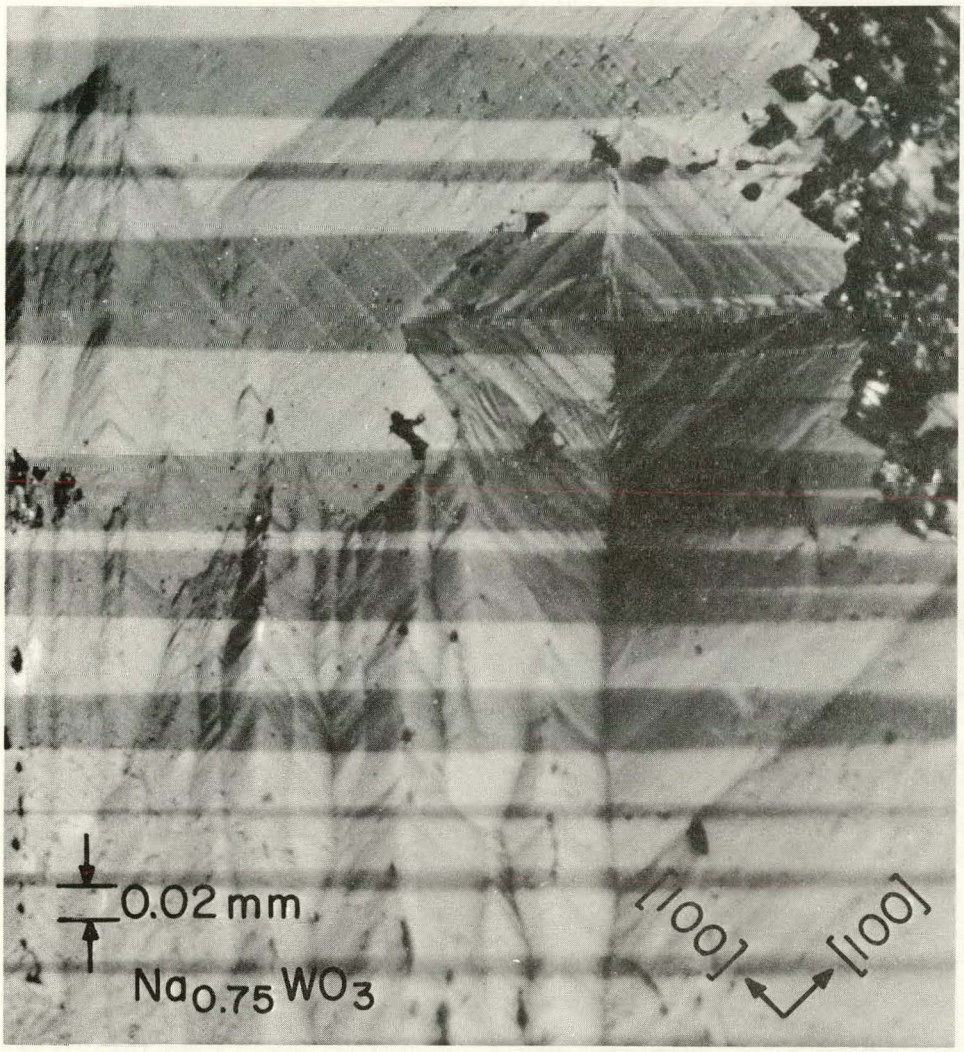

Fig. 9. Polarized-light Photomicrograph of an Electrolytically Synthesized Film Covering a Deeply Etched (010) Plane of $Na_{0.75}WO_3$. The morphological features of the etched substrate are visible because the film is translucent. The domain walls of the outermost film run parallel to the [110] axis. The surface was etched by the modified Murakami reagent and then subjected to anodic electrolysis in 10% NaOH solution for a few seconds at 0.1 mA/cm^2 and 5 V dc. ANL Neg. No. 122-78-274.

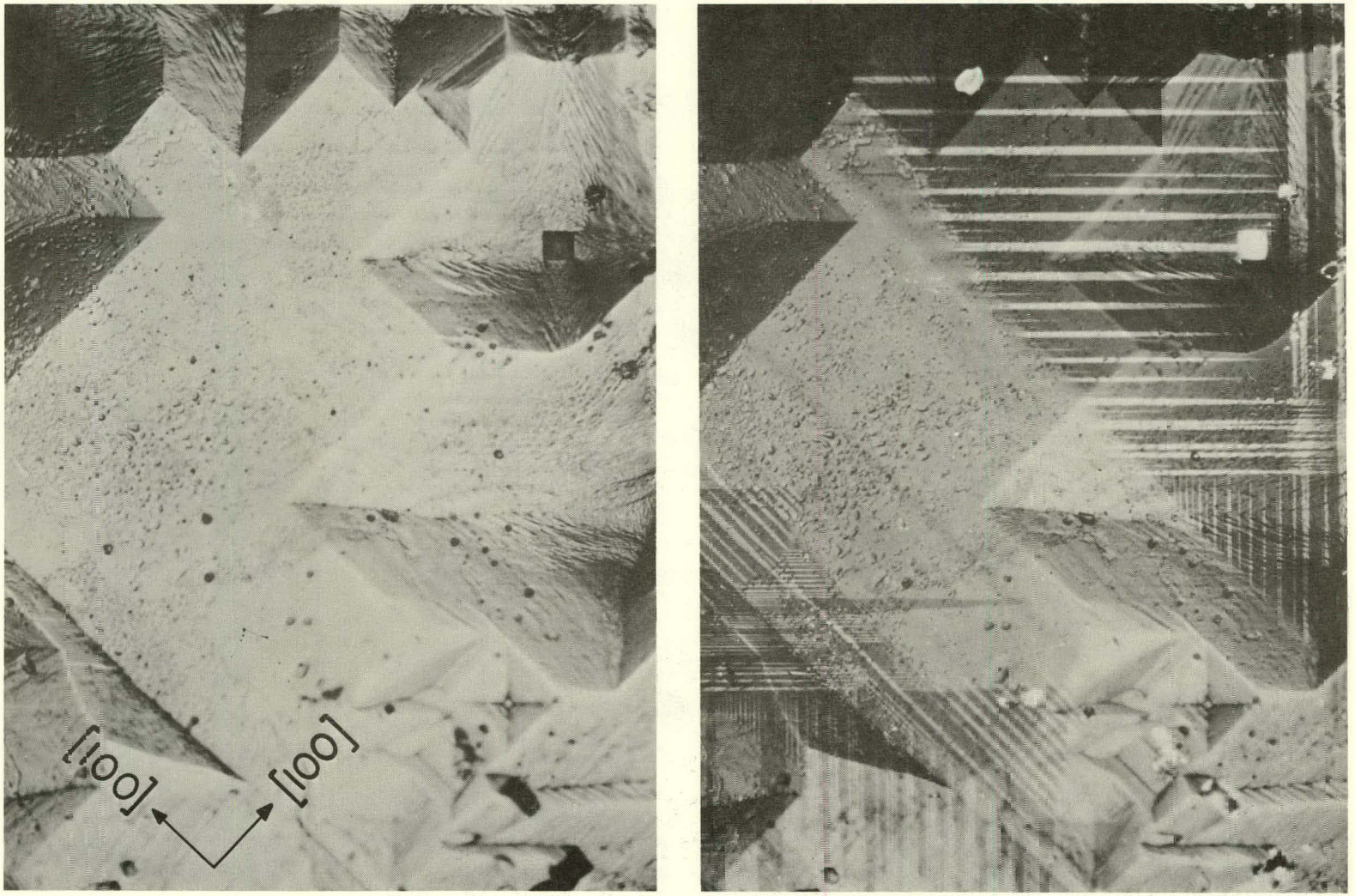

Fig. 10. Polarized-light Photomicrographs of Deeply Etched (010) Surface of $Na_{0.68}WO_3$ Covered with Surface Film. The birefringent contrast is minimum and maximum in (A) and (A'), respectively. In both (A) and (A'), the morphological features of substrate is clearly seen, because of the translucency of the film. The etching and the electrolysis procedures are the same as those in Fig. 9. ANL Neg. No. 122-78-342.

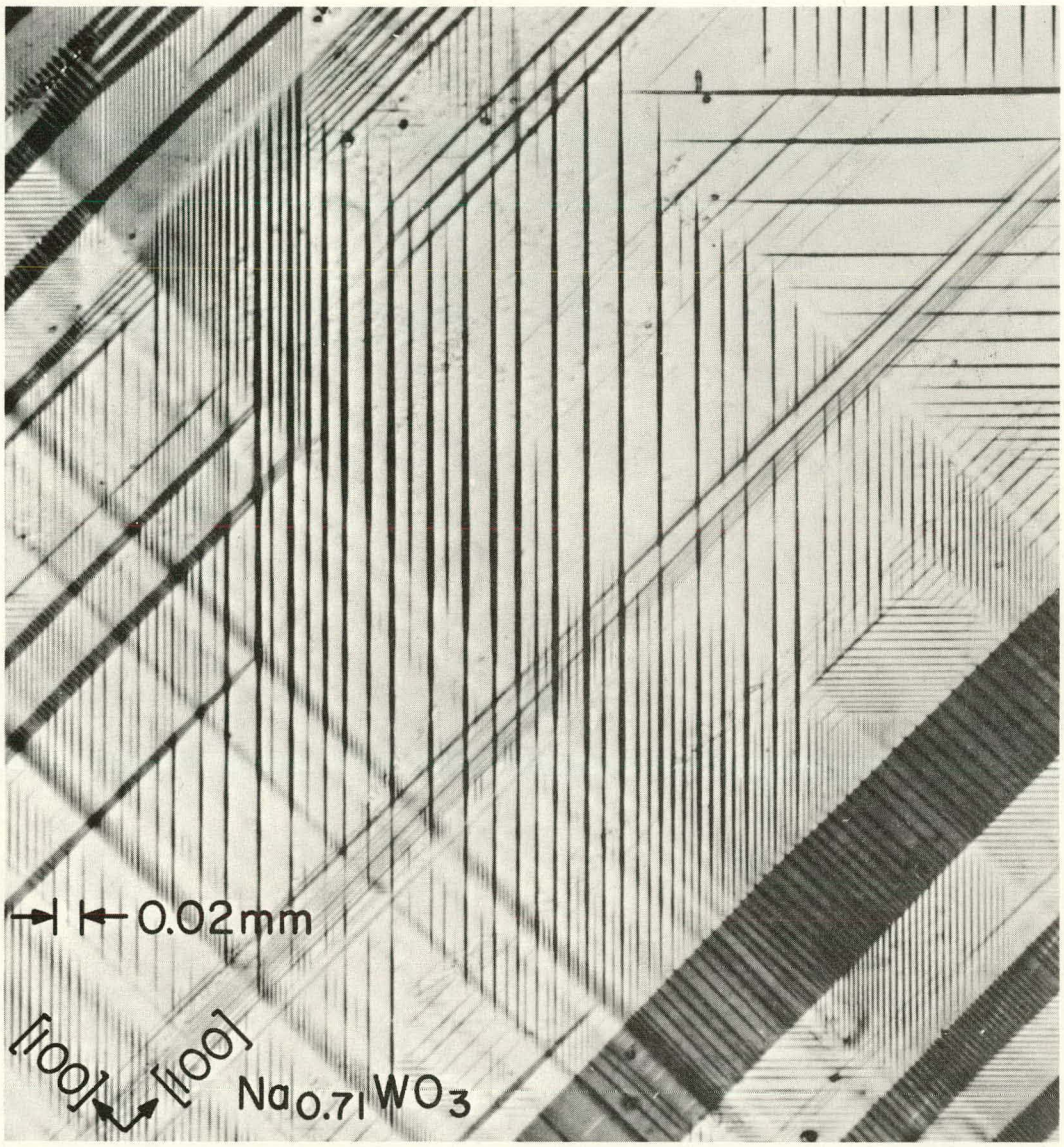

Fig. 11. Polarized-light Photomicrograph at Maximum Birefringent Contrast of Electrolytically Synthesized Surface Films on Polished (010) Plane of $Na_{0.71}WO_3$. Some surface blemishes are visible through the films. Several ⟨101⟩ stripes of the innermost film are vaguely seen. Detectability and contrast increase progressively for the outer films, namely, the ⟨100⟩ stripes of the second innermost film, the ⟨101⟩ stripes of the third film, the ⟨100⟩ stripes of the fourth film, and finally ⟨110⟩ stripes of the fifth and outermost film. Note that the domain stripes exhibit the needle-shaped ends and a bead-loop modulating width. ANL Neg. No. 122-78-271.

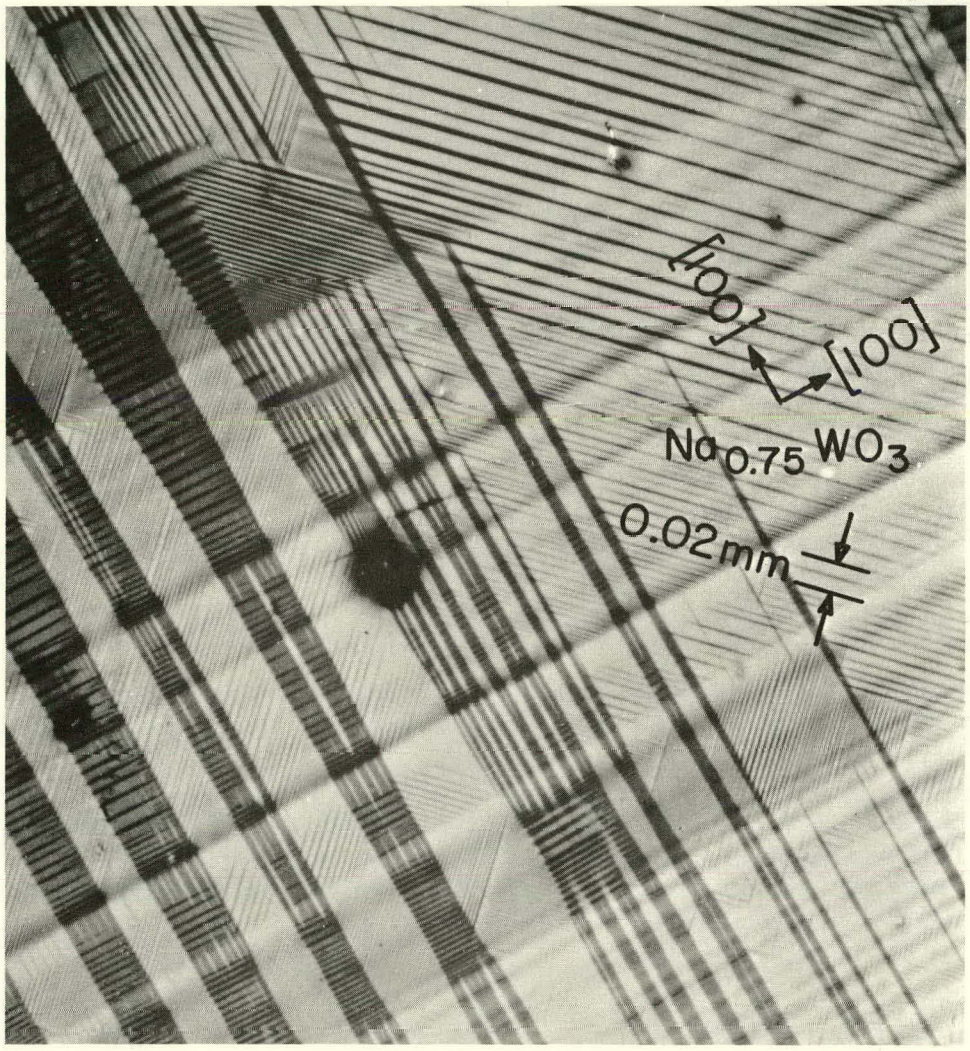

Fig. 12. Polarized-light Photomicrograph of Electrolytically Synthesized Surface Films on Polished (010) Plane of $Na_{0.75}WO_3$. Besides the domain characteristics similar to Fig. 11, broad twin bands show wedged and forklike domains. ANL Neg. No. 122-76-317A.

In the electrolytic synthesis of the film, the domain formation sometimes takes place a few minutes after the electrolytically treated surface is exposed to air. The domain formation is often slow enough to be perceived visually under the polarizing microscope. In some cases, the domains can be seen to form at one edge and then migrate to another edge of the surface. The propagation speed is about 0.1-1 m/s. Such a domain-forming process is also observed when the surface is wetted with alkaline solution in air. A similar process occurs on certain cleaved surface; that is, a freshly cleaved surface in moist air initially shows no domains, but develops the domained surface film a few seconds later.

During the preparation of the bronze crystals, the excess sodium tungstate in the final product is leached off in boiling water or hot NaOH solution. The sodium tungstate solution is strongly alkaline; hence the leaching process creates the film layer on the bronze surface as well as on the planar defects at which the cleavage may take place readily. The so-called freshly cleaved surface is often such a film-covered interface (see Sec. IV.C). Also, the virgin surface of the bronze has considerable affinity for water and probably also for oxygen (Wertheim et al., 1976), leading to the formation of the surface film.

An epitaxial correlation between the surface film and the substrate is shown by the following experiment. The bronze surface was polished and then electrolytically treated in an NaOH solution. The domain pattern of the surface film was photographed. A diamond paste was then used to polish the surface to remove the film. Then the surface was washed and electrolytically treated again. The main features of the domain pattern persisted (roughly 75%). The process was repeated three times on two different samples, with about the same results.

The (110) and (111) surfaces were also studied rather extensively. The electrolytic treatment and the etching processes yield neither well-crystallized surface film nor clearly definable morphological features. These aspects are represented by Figs. 13 and 14.

B. Structural Aspects

The twins form a variety of multiple stripes (as shown in Figs. 11 and 12). The single-domain width is roughly 0.001-0.01 mm in the orderly narrow stripes and as wide as 0.1 mm in the irregular broad ones. The narrow domains have been similarly observed in some ferroelectrics, e.g., $BaTiO_3$, Rochelle salt, and WO_3 (Jona and Shirane, 1962; Fatuzzo and Mets, 1967). As an illustration, we choose the substrate surface to be (010) and assume that the film is strain-free. In Tetragonal I, the median direction of the stripes in the first (innermost) film is parallel to either [101] or $[10\bar{1}]$ of the substrate. The stripes in the second film are parallel to either [100] or [001]. The stripes in the third film are the same as those in the first film, etc. Hence, the angle between the stripes in the neighboring film is 45 or 135°, while the stripes within a film can be mutually orthogonal.

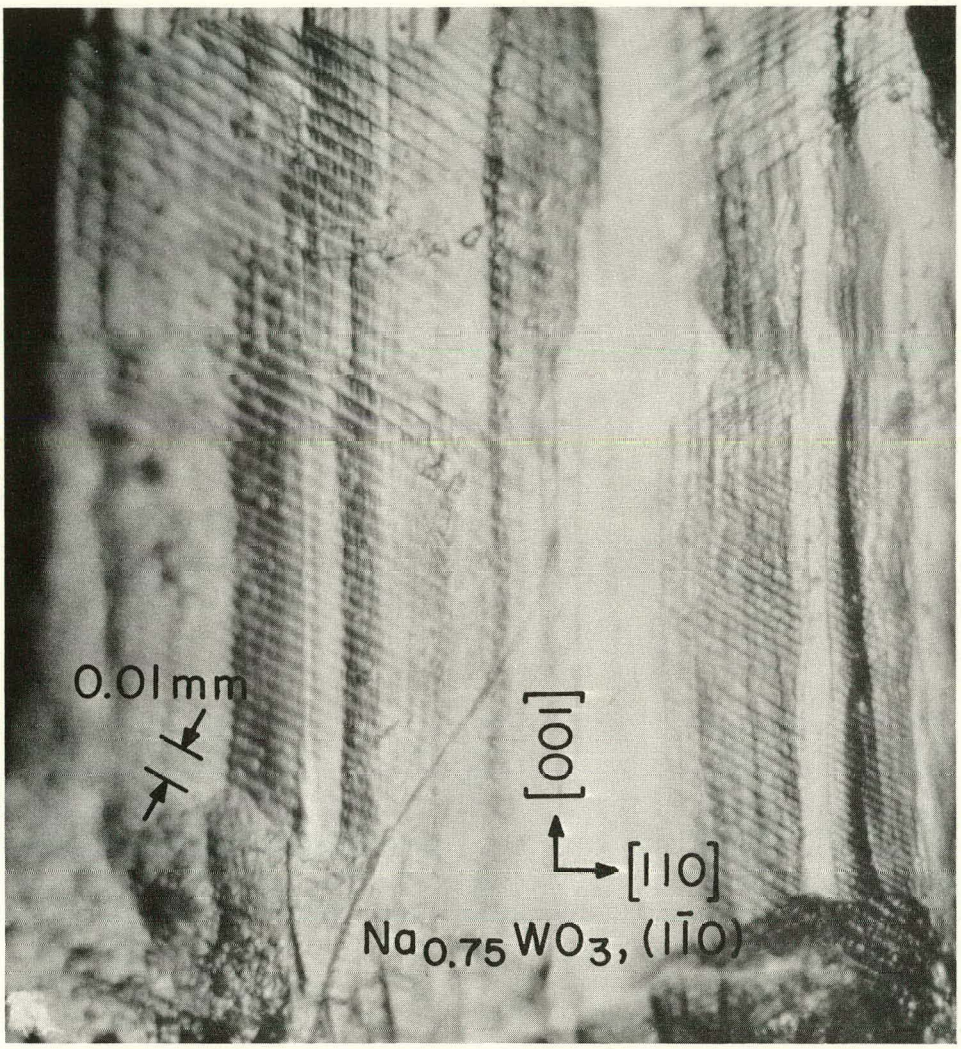

Fig. 13. Nomarski Interference-contrast Photomicrograph of Etched (110) Surface of $Na_{0.75}WO_3$. The striations are approximately parallel to [120], but gave no conclusive evidence for the possible [120] twinning. This surface shows vague birefringence. The etchant was a solution of 10% NaOH and 10% $K_3Fe(CN)_6$. ANL Neg. No. 122-77-953A.

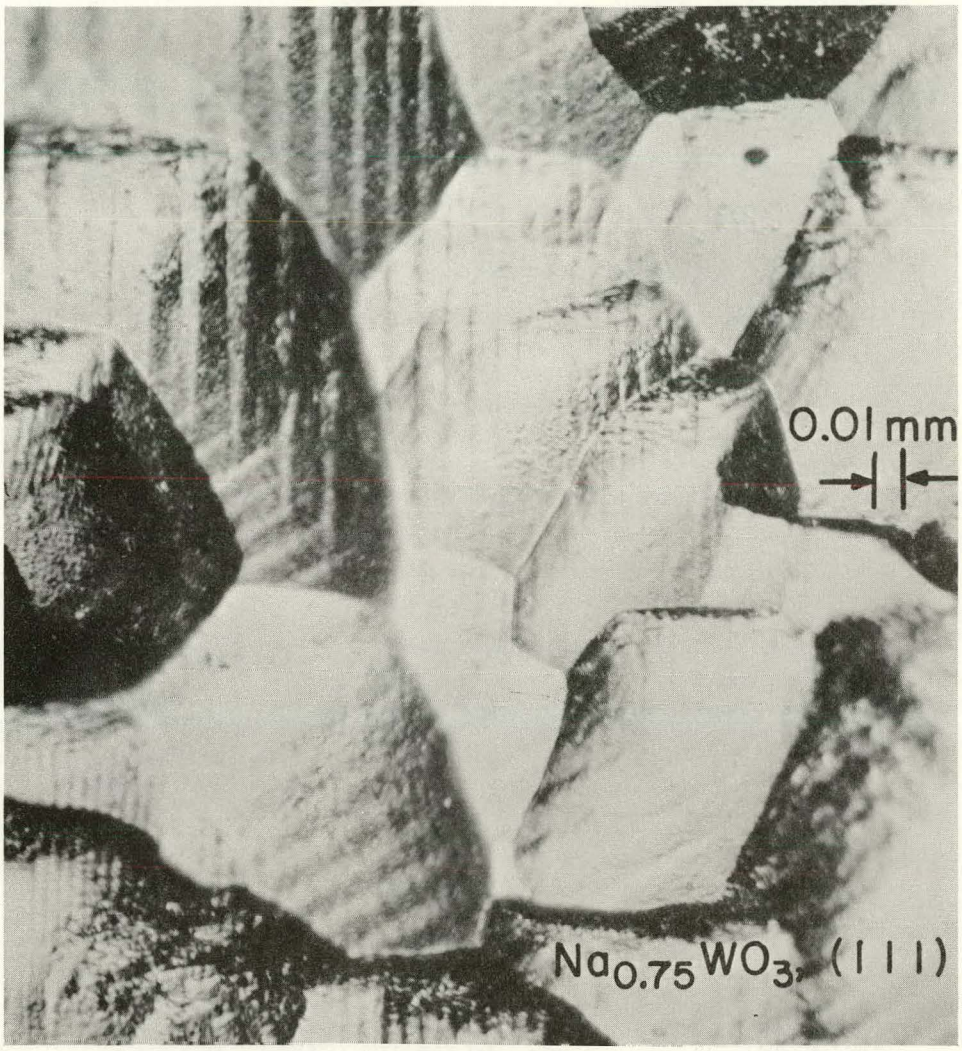

Fig. 14. Nomarski Interference-contrast Photomicrograph of Etched (111) Surface of $Na_{0.75}WO_3$. The morphology and the surface-film domains indicate the intersecting angles of 60 and 120°. The film shows a weak birefringence. The etching was performed using a solution of 10% NaOH and 10% $K_3Fe(CN)_6$. ANL Neg. No. 122-77-951A.

At the domain boundary, the optic axis of the domain rotates 90° about the axis perpendicular to the film layer. The angle between the stripes and the optic axis of the domain is 45 or 135° in the odd-number films and 0 or 90° in the even-number films. The film structure is probably pseudocubic tetragonal with the layer plane (010) and the optic axis [001]. The twinning plane is then {101} in the odd-number films and (100) or (001) in the even-number films.

The pseudocubic tetragonal structure of the film is further supported by the following observations:

1. The angle between the [100] and [001] domain walls is 90° (±0.1°). The terminal angle of the needlelike domain gives $2 \tan^{-1}(c/a) \simeq 89.9°$; hence, $c/a \simeq 0.997$.

2. If the structural anisotropy in the (101) plane is large, then the energy of formation of the (100) plane is significantly different from that of the (001) domain. Hence, the population difference between the (100) and (001) domains should be readily detectable. This appears contrary to observation; therefore the tetragonal anisotropy should be very small.

3. The strain energy associated with the simultaneous existence of the (100) and (001) domains is reduced by the formation of the wedge-shaped domains. However, if these two types of domains cannot be made to fit tightly in the wedge formation, then microcracks would have developed between the domain blocks (each of which contains one type of domain). No such interblock microcrack has been observed, implying that the domain-wall formation is subjected to a very small anisotropy.

The film structure is further characterized as a pseudocubic perovskite type having various tilting modes of oxygen octahedra. A displacement of sodium from the corner of the pseudocubic cell is also possible. These distortions and displacements should be very small, comparable to the amplitudes of thermal vibration. In other words, the energy required for distorting the perovskite structure is roughly equal to the phonon excitation energy in thermal vibration. This is a major reason for instability of the domain configuration of the film (see Secs. IV.D and IV.E below).

The thickness of the domain wall is presumably of the order of the lattice constant as found in ferroelectrics (Jona and Shirane, 1962) and hence is much thinner than the ferromagnetic domain wall, whose thickness is several hundred lattice constants.

Selected references regarding the film structure are as follows: For a review on the tungsten compounds, see Rieck (1967). For general discussions on the mechanical twinning, see Hall (1954), Reed-Hill et al. (1964), Klassen-Neklyudova (1964), and Reid (1965). Regarding the perovskite and its modified

structures, see Galasso (1969), Hyde and O'Keeffe (1973), Polaczkowa and Polaczek (1974), Glazer (1975), and Hussain and Kihlborg (1976). The lattice vibration in the bronze has been discussed by Scott and Leheny (1970), Kamitakahara et al. (1976), and Flynn et al. (1978).

Representative studies on WO_3, reduced WO_3, and their crystallographic-shear structures are by Ebert and Flasch (1934 and 1935), Glemser and Sauer (1943), Ueda and Ichinokawa (1951), Nakamura (1956b), Sawada (1956a and 1956b), Sawada and Danielson (1959a, 1959b, and 1959c), Tanisaki (1959a and 1959b), Gadó (1965), Spyridelis et al. (1967), Amelinckx and Van Landuyt (1970), and Loopstra and Boldrini (1966).

For the tetragonal structure of Na_xWO_3 with small x, see Magnéli (1949b) and Takusagawa and Jacobson (1976). Concerning the hydrogenated bronze structure, see Glemser and Naumann (1951), Mitchell (1963), Wiseman and Dickens (1973), and Hoppmann and Salje (1976). In this context, it is of interest to quote the crystal data of two representative hydrated tungsten oxides: tetragonal $W_4O_{10}(OH)_2$(= 4 $H_{0.5}WO_3$) with a = 3.79 and c = 3.74; tetragonal $W_{12}O_{32}(OH)_2$(= 12 $H_{0.167}WO_{2.833}$) with a = 3.85 and c = 3.65 Å (Glemser and Naumann, 1951). For comparison, the reduced-unit-cell dimensions of $Na_{0.50}WO_3$, $Na_{0.75}WO_3$, and the hypothetical $NaWO_3$ are 3.826, 3.846, and 3.867 Å, respectively.

C. Properties

The surface film is chemically more inert than the bulk crystal. The domain structure was uninfluenced by hot concentrated HCl, HNO_3, HF, H_2O_2, and various admixtures thereof. Concentrated H_2SO_4 did modify the domain structure about 30%, probably due to a dehydration of the film, since various mixed solutions of H_2SO_4, HCl, HNO_3, and H_2O_2 showed no such effect. In these experiments, the samples had to be handled carefully, since the domain is modulated by slight pressure such as gentle priming with the finger (see Sec. IV.D).

The film, unlike WO_3, is inert to boiling NaOH, KOH, NH_4OH, Na_2O_2, H_2O_2, and various admixtures thereof. A similar inertness was observed with reducing reagents, such as sodium sulfite and hydroxylamine hydrochloride. Liquid metal polishes of commercial sources were also ineffective.

The domain is uninfluenced by anodic and cathodic electrolyses in acids and by cathodic electrolysis in alkaline solutions. The anodic electrolysis in alkaline solution dissolves the bronze continuously, maintaining an equilibrium thickness of the surface film (Šepa et al., 1974). Electron diffraction in the bronze foil prepared by this method indicated that the outer atomic layers of the surface film are largely dielectric, thereby deflecting away most electrons. Probably the only way to remove the film is by mechanical polishing. A 0.25-μm diamond paste (Tegart, 1959) was used routinely for this purpose.

Note that the surface film can exist only epitaxially (or parasitically) and cannot be isolated from the substrate. The equilibrium thickness of the film would become dependent on the size and the shape of the substrate when the substrate is smaller than a certain critical size. The unmodulated surface of the bulk crystal should be considerably reactive because of the sodium atoms being exposed to the surface. This high reactivity is suppressed greatly by forming the surface film. The reactivity can also be suppressed by a successive degression of the sodium concentration in the outer-surface layers of the substrate.

The bronze single crystal exhibits the cleavage parallel to the {100} planes. As pointed out in Secs. III and IV.A, the cleavage may not be an intrinsic bulk property. This view is further supported by the domain structure of the film covering the cleaved surface. Figure 15 shows the matched pair of the cleaved surfaces. The film domains of the as-cleaved pair, A_1-A_1', are not well crystallized. The anodic electrolysis in 10% NaOH solution purified and recrystallized the film as indicated by well-defined domain pattern in the A_2-A_2' pair. In both cases, roughly 60-75% of the domain patterns of the matched pair are identical. Both faces exhibit the double-layer films. The cohesive stacking is realized between the film with the ⟨100⟩ domains and the film with the ⟨110⟩ domains. However, the domains of the outermost film of A_1 and those of A_1' are the same ⟨110⟩ types, resulting in the repulsion between A_1 and A_1', hence the cleavage.

The cleaved surface is generally expected to be smoothly flat, not as jagged as shown in Fig. 16. This observation presents additional support to the proposition that the cleavage of the bronze is caused by structural imperfection.

The effect of hydration in the film was examined as follows. The domain pattern of the wet film is fuzzy, but becomes sharply defined when the film is dried at about 60°C. This means that some water molecules are so loosely bound to the film that they can be driven off at about 60°C. The reproducibility of the domain configuration of the film in the pyrostrictive modulation (see Sec. IV.D) is higher for the higher temperature used for drying the film. When the film is dried at 60 and 300°C, the reproducibility is about 75 and 95% in the first-cycle pyrostrictive modulation below 60 and 300°C, respectively. When the dried film is wetted with water, the water molecules are absorbed and the domain pattern becomes fuzzy. When the film is heated above 350°C, oxidation becomes appreciable. Above 400°C, the surface is covered with blue metallic-lustre film (WO_3). In all cases mentioned above, heating was performed in air for about 1 min.

The electrical conductivity of the bulk crystal is not significantly influenced by the formation of the surface film. This resembles Al_2O_3 on aluminum metal, exhibiting a fast electronic tunneling through the oxide layer in the electric conduction (Diggle, 1972 and 1973).

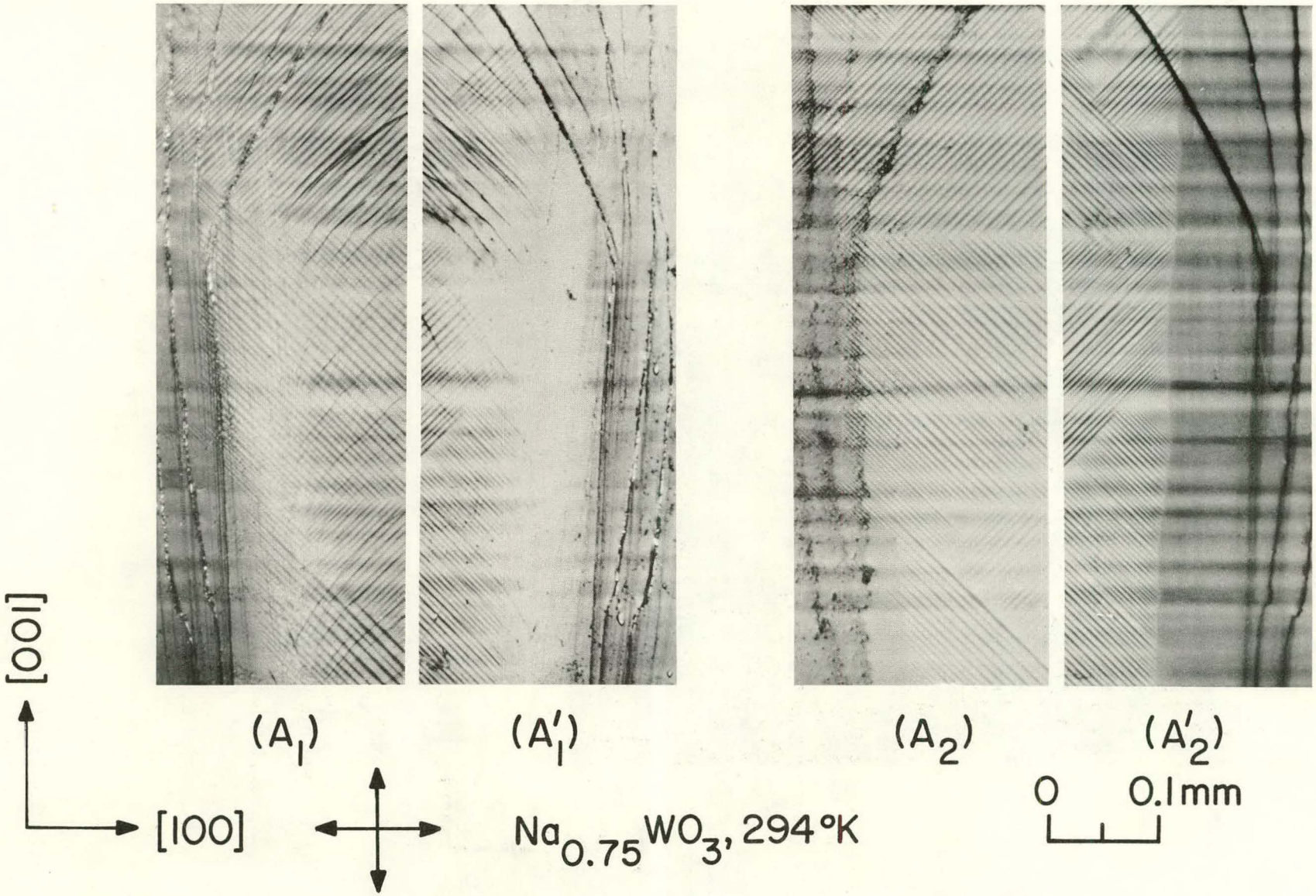

Fig. 15. Polarized-light Photomicrographs of Matched Pair of Cleaved (010) Surfaces of $Na_{0.75}WO_3$. The as-cleaved (010) faces are shown in A_1 and A_1'. The same pair after being treated electrolytically are displayed in A_2 and A_2'. The crossed arrows indicate the directions of the polarization vectors of the polarizing and analyzing Nicols. The film domains on these cleavage surfaces suggest that the cleavage is due to a growth imperfection and is not an intrinsic bulk property. ANL Neg. No. 122-78-508A.

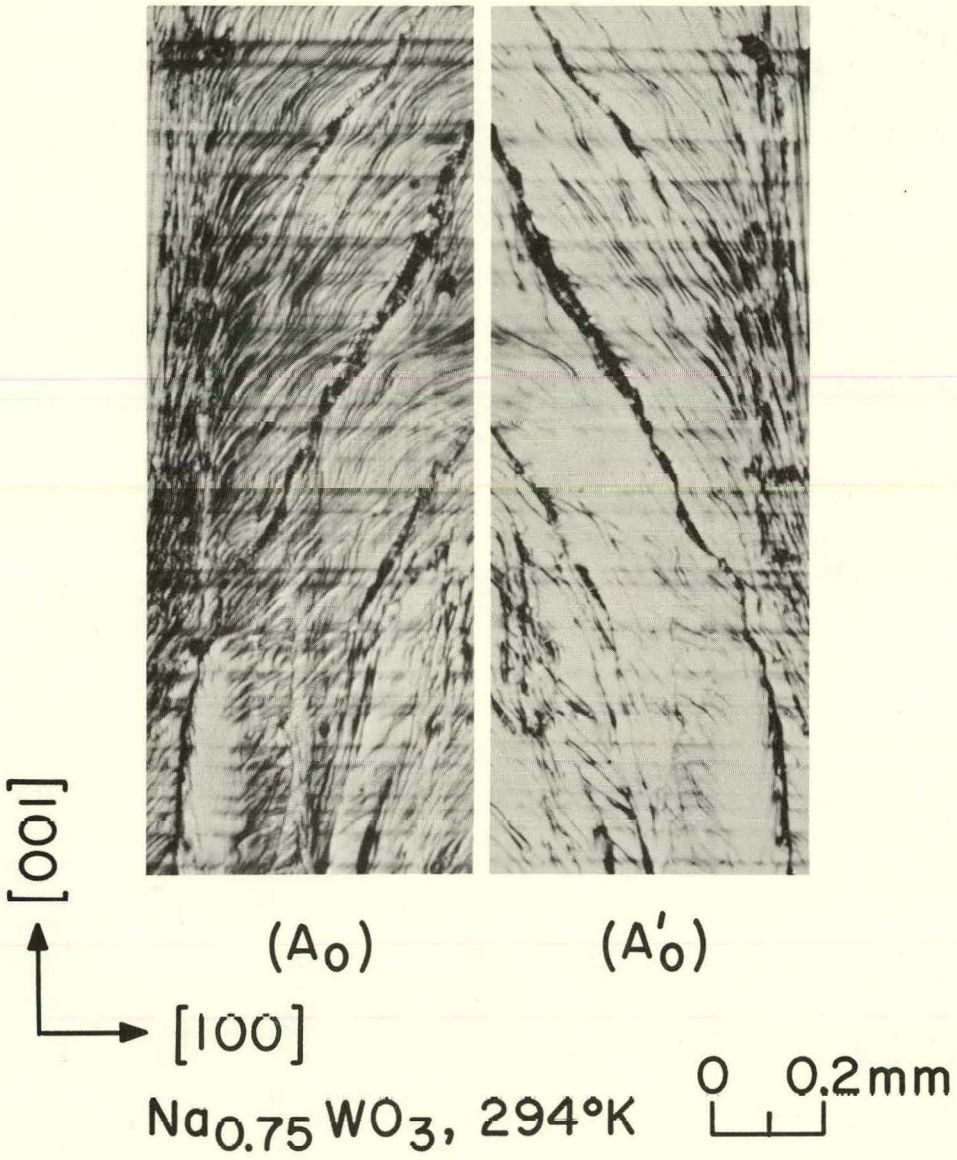

Fig. 16. Unpolarized-light Photomicrographs of Matched Pair of Cleaved Surfaces of $Na_{0.75}WO_3$. The substrate is covered with the surface film, which is not seen because of nonbirefringency in unpolarized light. The surface is too jagged to be the usual cleavage plane. ANL Neg. No. 122-78-509.

D. Effect of Temperature

Table I summarizes the temperature-dependent physical properties governing the phase-transition region (from about -50 to 300°C). Figure 17 shows the transition temperatures reported in the literature. Figure 18 displays the temperature dependency of the lattice parameters of a representative bronze ($Na_{0.81}WO_3$) and the proposed crystal-structure data, all reported by Clarke (1977). The phase-transition data obtained by the recent Raman scattering experiment (Flynn et al., 1978) are almost identical to Clarke's data (1977).

The T_1 transition was detected in optical, X-ray, and Raman measurements, but was undetected in more than a dozen other physical measurements. The discrepancy between Ingold and DeVries (1958) and Clarke (1977) is larger at lower values of x, e.g., as much as 20°C at $x = 0.8$. Optical measurements of Atoji (1978) agree with Clarke's data (1977). Our recent neutron-diffraction data indicated a larger tilting of oxygen octahedra at lower temperatures, but no detectable change at T_1. The heat-capacity curve (Inaba and Naito, 1975) shows a small slope change at T_1.

The T_2 transition discovered by Clarke was confirmed by Flynn et al. (1978) and also by Atoji (1978). Ingold and DeVries (1958), as well as many other investigators, did not detect the T_2 transition.

Unlike T_1 and T_2, the T_3 transition was found by almost all methods. The T_3 values obtained by Ingold and DeVries (1958) agree with those of Clarke (1977), but differ as much as 30-80°C from those reported by Rosen et al. (1956b) and Shanks and Redin (1966).

Clarke (1977) postulated that, on the basis of his proposed space groups, T_1 and T_2 are of first order because of the transition between the nonsubspace groups, while T_3 is of second order because of the transition between the subspace groups. Note that all these space groups are centrosymmetric and are not piezo- or pyroactive. Although these postulations have been neither fully confirmed nor eliminated, the available data so far do not contradict the transition schemes proposed by Clarke (1977). For example, the lattice parameters change discontinuously at T_1 and T_2, but continuously at T_3. On the other hand, the thermal-expansion coefficient hardly changes at T_1 and T_2, but significantly at T_3, in agreement with other thermal properties.

X-ray (Clarke, 1977), Raman (Flynn et al., 1978), and NMR (Bonera et al., 1971) measurements indicate that T_3 is a second-order transition inducing a noncubic distortion to the perovskite structure which is stable above T_3. On the contrary, the heat-capacity data (Inaba and Naito, 1975) imply the higher-temperature phase to be more disordered.

The T_3 transition was observed in the thermal conductivity (Shanks and Redin, 1966) but not in the electric resistivity (Ellerbeck et al., 1961), although

TABLE I. A Survey of Temperature-dependency Measurements on Various Physical Properties of the Sodium-Tungsten Bronzes. Quoted are the data in the temperature range from about -40 to 250°C governing the transition temperatures, T_1, T_2, and T_3 (Clarke, 1977).

Method and Crystal Form	Temp. Range, °C	x in Na_xWO_3	Transition Temperature Detected			Reference
			T_1	T_2	T_3	
X-ray lattice parameter: powder	20-600	7 x's, 0.300-0.845	No	No	Yes	Rosen et al. (1956b)
X-ray lattice parameter: single crystal	-30-230	0.62, 0.81, 0.94	Yes	Yes	Yes	Clarke (1977)
Dilatometry: powder	20-600	0.8		No	Yes	Takamori and Tomozawa (1964)
Optical microscopy: single crystal	-40-200	16 x's, 0.52-0.93	Yes	No	Yes	Ingold and DeVries* (1958)
Optical microscopy: single crystal	-40-200	5 x's 0.6-0.9	Yes	Yes	Yes	Atoji (1978)*
Raman spectroscopy: single crystal	-269-227	5 x's 0.51-0.94	Yes	Yes	Yes	Flynn et al. (1978)
Heat capacity: powder	-258-27	0.679	No			Gerstein et al. (1964)
Heat capacity: powder	27-627	0.485, 0.698, 0.794	**	No	Yes	Inaba and Naito (1975)
Differential thermal analysis: powder	27-497	0.8		No	Yes	Taylor and Weller (1970)
Thermal conductivity: single crystal	77-527	0.513, 0.804			Yes	Shanks and Redin (1966)
Magnetic susceptibility: single crystal	-203-27	0.49, 0.76, 0.86	No			Greiner et al. (1962)
NMR: single crystal	-173-427	0.517, 0.72, 0.855	No†	No	Yes	Bonera et al. (1971)
Seebeck effect: single crystal	-269-27	7 x's 0.512-0.875	No			Muhlestein and Danielson (1967a)
Hall effect: single crystal	-196-96	13 x's, 0.605-0.865	No	No		Gardner and Danielson (1954)
Hall effect: single crystal	-269-27	17 x's 0.4-0.9	No			Muhlestein and Danielson (1967b)
Hall effect: single crystal	-272-27	0.26, 0.3, 0.6	No			Lightsey (1973)††
Electrical resistivity: single crystal	-263-27	13 x's 0.605-0.865	No			Gardner and Danielson (1954)
Electrical resistivity: single crystal	-269-600	12 x's 0.49-0.88	No	No	No	Ellerbeck et al. (1961)
Electrical resistivity: single crystal	-269-27	17 x's 0.4-0.9	No			Muhlestein and Danielson (1967b)
Electrical resistivity: single crystal	-272-27	5 x's 0.22-0.63	No			Lightsey (1973)††

*These measurements were made on the epitaxial surface films.

**The heat-capacity curve shows a small change of slope near T_1.

†The NMR data by Bonera et al. (1971) and those by Tunstall (1975) indicate that the noncubic structure persists down to 1.6 K.

††The so-called cubic range could be extended down to about x = 0.22 by depleting sodium atoms nondestructively from a $Na_{0.6}WO_3$ single crystal using a diffusive dilution method. See also Lightsey et al. (1976).

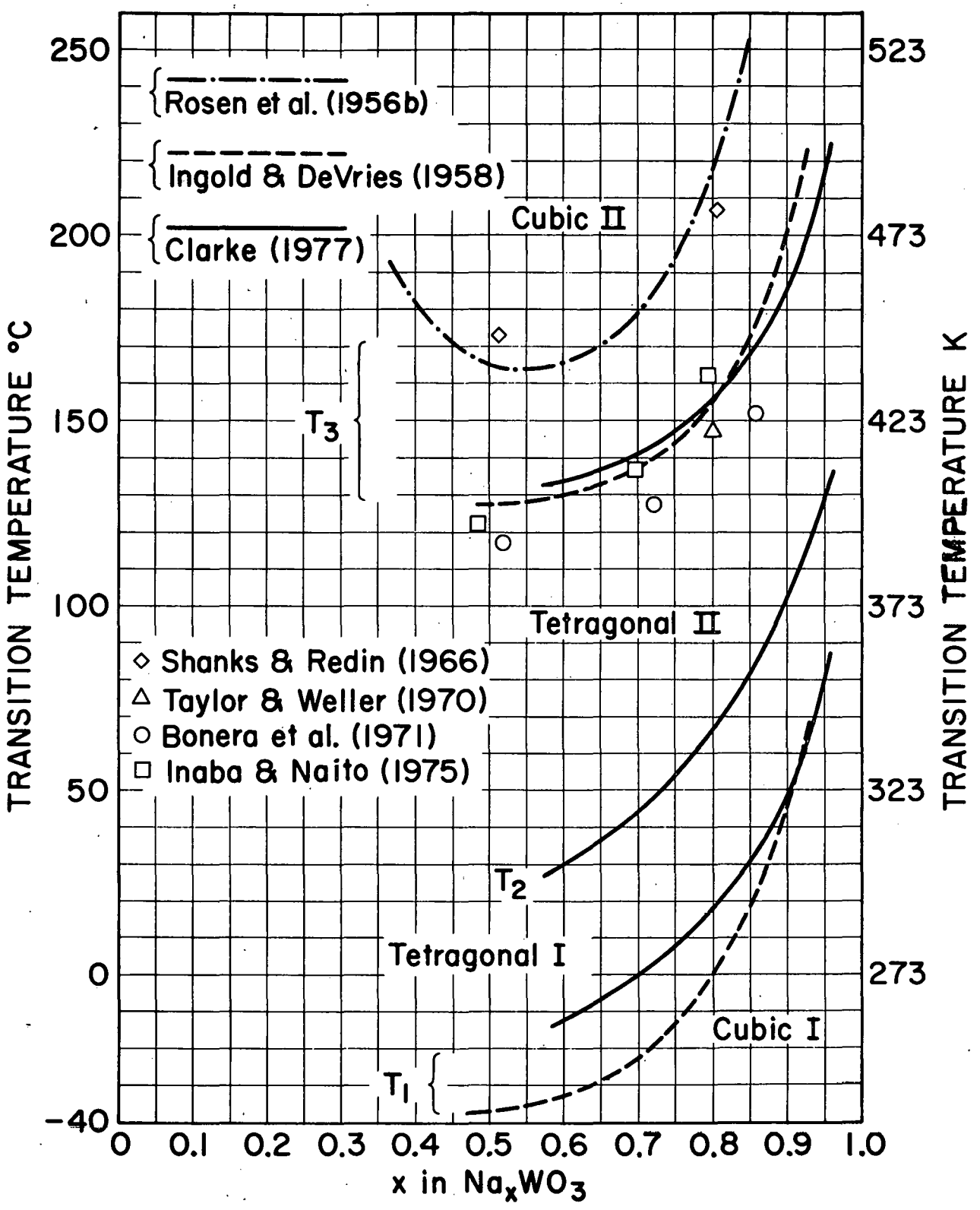

Fig. 17. Transition Temperatures of Pseudocubic Na_xWO_3, $0.35 < x < 1$. The data of Rosen et al. (1956), Ingold and DeVries (1958), and Clarke (1977) are represented by the interpolated curves, because of many available experimental points. All other data are given by individual experimental points. ANL Neg. No. 122-78-281.

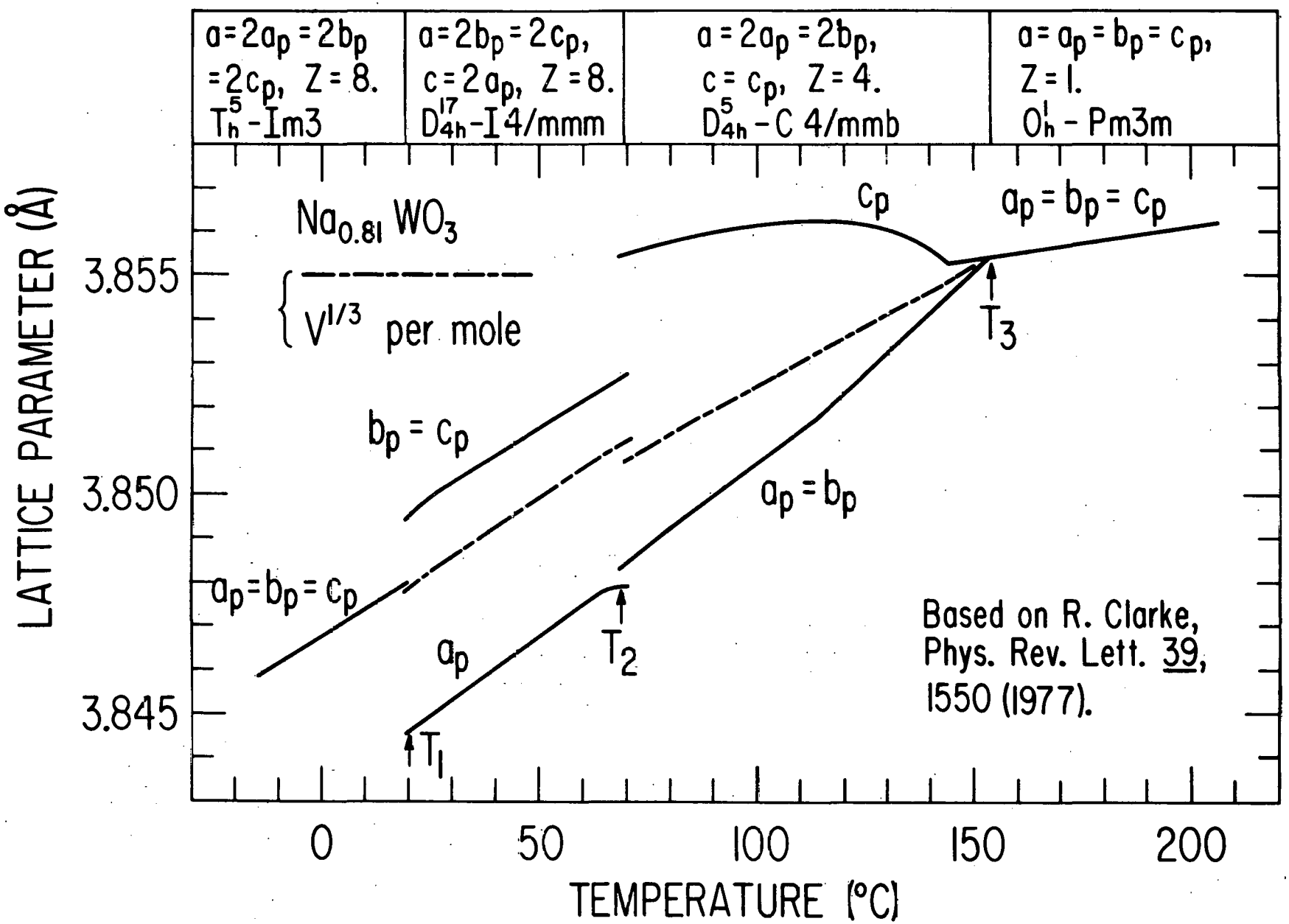

Fig. 18. Temperature Dependencies of Lattice Parameters and Crystal Structures of Four Structural Phases of $Na_{0.81}WO_3$. All data are based on Clarke (1977). The lattice parameters are shown in terms of the reduced pseudocubic unit-cell dimensions, a_p, b_p and c_p. The space-averaged linear thermal expansion in the tetragonal region is given by $V^{1/3}$ (V = molar volume). ANL Neg. No. 122-73-365.

these transport properties are similarly phonon-related. In any event, improved measurements are required on practically all physical properties of the bronzes.

The temperature dependencies of the domain structure of $Na_{0.70}WO_3$ and $Na_{0.6}WO_3$ are shown in Figs. 19 and 20. In Fig. 19 the film domain appears to monitor the phase transitions of the $Na_{0.70}WO_3$ substrate at $T_1 = 9°C$, $T_2 = 52°C$, and $T_3 = 148°C$, reported by Clarke (1977). At 0°C, the film structure is nearly isotropic (the substrate is Cubic I); at 13°C, the ⟨101⟩ domains dominate (Tetragonal I); at 23°C, the population change occurs among the $[10\bar{1}]$ and [101] domains (Tetragonal I); at 57°C, the ⟨100⟩ domains start to appear (the transient state between Tetragonals I and II); at 63°C, the ⟨100⟩ domains dominate (Tetragonal II); at 90°C, the population change takes place among the [100] and [001] domains (Tetragonal II); at 110°C, a further population change occurs among the [100] and [001] domains (Tetragonal II); at 150°C, the film becomes isotropic (Cubic II).

In Fig. 20, the transition temperatures of $Na_{0.6}WO_3$ are $T_1 = -13°C$, $T_2 = 30°C$, and $T_3 = 133°C$ (Clarke, 1977). The domain of the surface film changes in an apparent coherence with the structural change of the substrate. The ⟨101⟩ domains at 23°C (the substrate being Tetragonal I) are replaced by the ⟨100⟩ domains at 35°C (Tetragonal II). The thermoelastic effect changes the optical reflectivity, but not the domain configuration as shown by the 71°C pattern (Tetragonal II). The film becomes isotropic at 140°C (Cubic I). The domain pattern at 23°C is similar to that of Rochelle salt (Fig. 4 of Mitsui and Furuichi, 1953).

Within Tetragonals I and II, the temperature change causes a gradual alteration on the domains, but without rotatory change of the domain wall. The domain appears to be modulated epitaxially by such small factors as thermal expansion of the substrate. Hence, the phase transition of the substrate is accompanied by a drastic change in the domain configuration of the surface film. In addition to the anisotropic-isotropic transformation of the film at the tetragonal-cubic transition of the substrate, we found that, in the vicinity of the Tetragonal I-II transition, the film domain changes markedly and the twinning planes undergo a rotatory shift of 45 or 135°. Consequently, in Tetragonal II, the first film contains the [100] and [001] walls, the second film contains the $[10\bar{1}]$ and $[\bar{1}01]$ walls, etc. The orientation of the domain walls of the innermost film often coincides with the striation pattern of the sodium segregation in the substrate (see Sec. III). The domain modulation by temperature change is occasionally accompanied by an audible, high-pitched, snapping sound ("cry of tin" or Barkhausen sound).

The surface-film domain is often unrelated to the pseudodomain and other morphological features of the substrate (see Sec. III). Moreover, we found that morphological and optical properties of the substrate do not change at the reported phase transitions. Accordingly, the optical microscopy

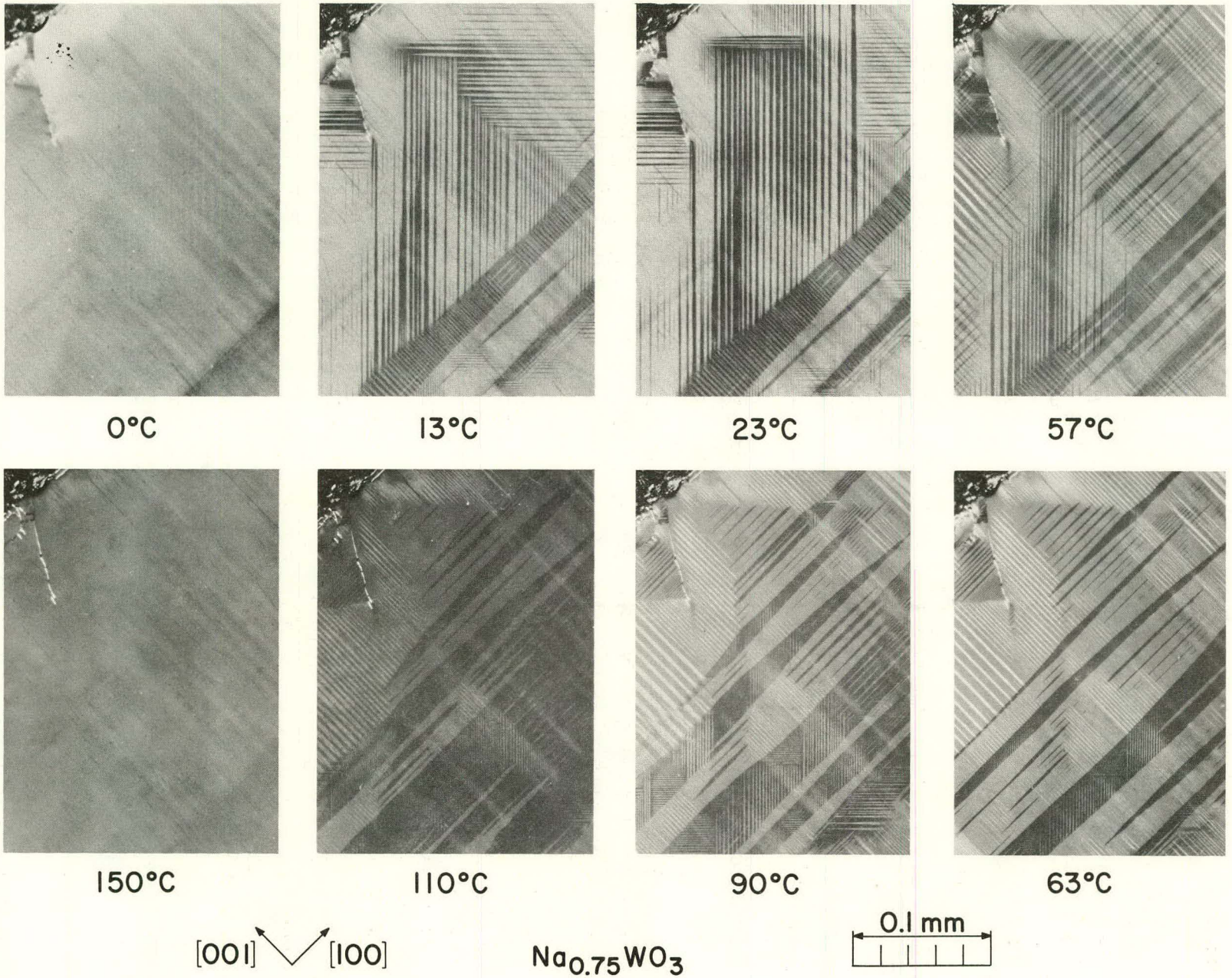

Fig. 19. Polarized-light Photomicrographs Showing Temperature Dependency of Domain Structure of Surface Film of $Na_{0.70}WO_3$ at 0-150°C. ANL Neg. No. 122-78-306.

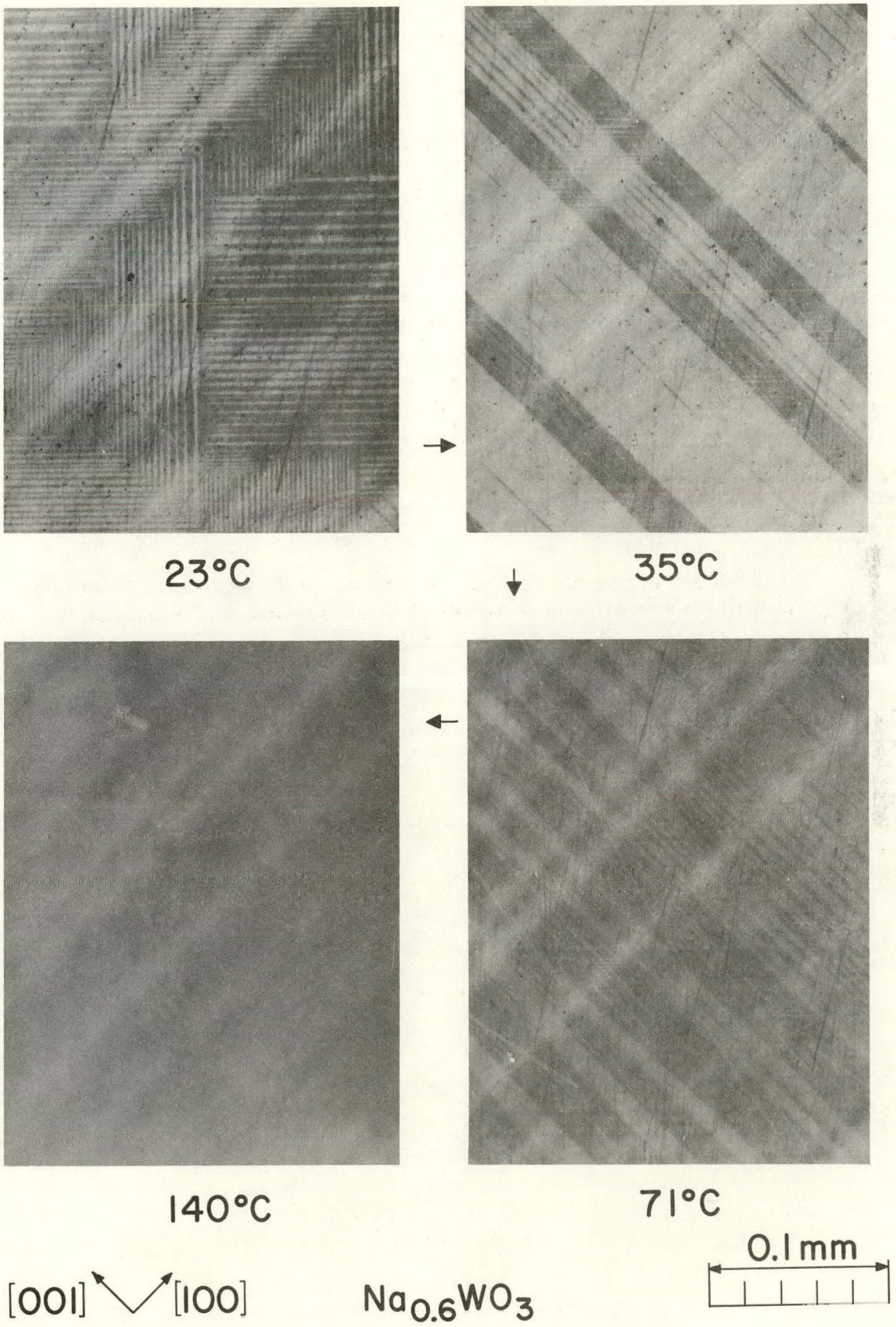

Fig. 20. Polarized-light Photomicrographs showing Temperature Effect on Surface Film of $Na_{0.6}WO_3$ at 23-140°C. ANL Neg. No. 122-78-307.

was unable to establish whether the modulation of the film domain is independent of, or dependent on, the structural change of the substrate.

E. Effect of Pressure

As observed in $BaTiO_3$ (Kay, 1948), WO_3 (Ueda and Ichinokawa, 1951), and Rochelle salt (Mitsui and Furuichi, 1953) the domain boundaries are modulated by any feeble lateral stress, such as a gentle touch with tweezers.

The pressure effect is approximately inversely proportional to the angle between the direction of the applied pressure and the median direction of the domain walls. Consequently, the domain walls parallel to the applied pressure diminish at a lesser pressure than that required to diminish the domain walls perpendicular to the pressure (see Fig. 21). In other words, at an initial stage of compression, most parallel walls disappear, and a single-domain size of 3×10^{-2} cm in linear dimension can be readily produced. This is followed by a gradual decrease of the perpendicular and 45° walls. When the pressure is removed, the domains reappear and reconstitute in average about 75% of the original pattern.

The boundary migration induced by the stress is usually perceptible visually, and the migration is estimated to be about 0.1-1 m/s (cf. 0.2 cm/s in Rochelle salt, Mitsui and Furuichi, 1953).

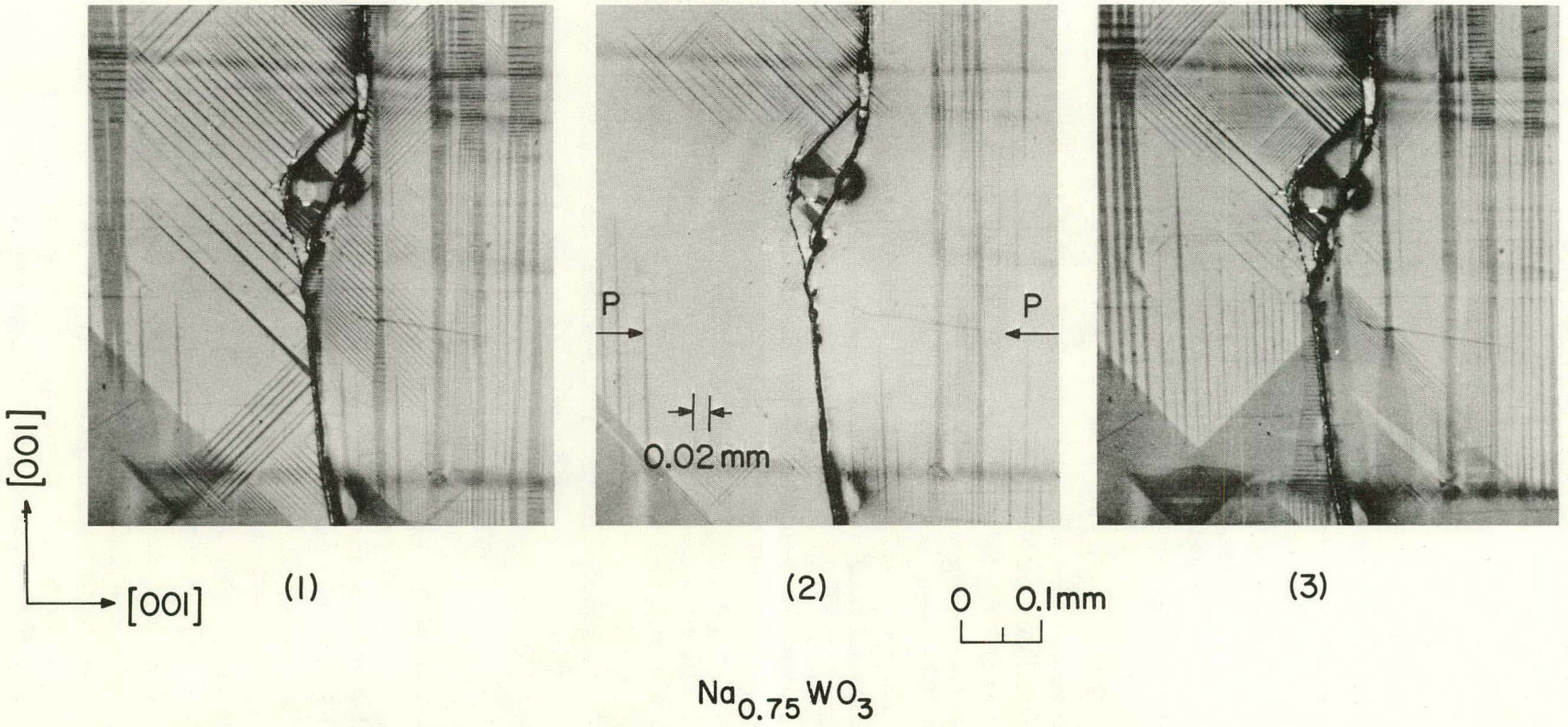

Fig. 21. Polarized-light Photomicrographs Showing Effect of External Pressure on Domain Structure of Surface Film of $Na_{0.75}WO_3$. (1) The original state (zero applied field). (2) The external pressure is being applied parallel to the [001] axis. Most domain walls are diminished. (3) The pressure is released, and the original structure is mostly reproduced. The surface under pressure is being deformed cylindrically. The cylindrical axis lies underneath and parallel to the surface and is perpendicular to the pressure. ANL Neg. No. 122-78-344.

V. ELECTRONIC SPECTROSCOPY, MICROSCOPY, AND DIFFRACTION

A. X-ray Photoelectron Spectroscopy

X-ray photoelectron spectroscopy (XPS) was used for a further characterization of the bronze surface. The XPS data of WO_3, WO_2, and Na_2WO_4 were also obtained for comparison (cf. Campagna et al., 1975; Colton and Rabalais, 1976; DeAngelis and Schiavello, 1976 and 1977; Wertheim et al., 1976; Chazalviel et al., 1977). Photoelectron spectra were recorded with a McPhearson ESCA 36 spectrometer using Mg Kα (1253.6-eV) radiation. Samples were maintained in a vacuum of 10^{-7}-10^{-8} Torr during analysis. The escape depth (thickness from which half the photoelectron intensity is derived) is about 10 Å in our tungsten compounds (see Carlson, 1975; McGuire and Carlson, 1972/73).

Several samples were cut from a large $Na_{0.75}WO_3$ single crystal. The first set of samples was polished and then cleaned using organic solvents and water. The second set of samples was polished, electrolytically etched in 10% KOH solution, and then washed thoroughly with water. All these samples showed the twinned surface film and essentially the same XPS data. The photoelectron peak for the Na(1s) level is very weak, only about 10 counts/s, implying a large depletion in sodium.

The O(1s) photoelectrons gave partially overlapped peaks at the binding energies of 530 and 532 eV, with about 160 and 40 counts/s for the intrinsic and extrinsic oxygen atoms, respectively. The intrinsic atoms comprise the regular crystal structure. The extrinsic atoms belong to abnormal structures such as defects and surface layers, or to adsorbed molecules. The width of the extrinsic O(1s) peak is broader, owing to the variety of chemical bondings involved. The tungsten 4f level yielded three peaks having the binding energies, 37.6, 35.5, and 33.4 eV, with an intensity ratio of about 5:9:2, respectively. The first peak is assigned to W^{6+} $4f_{5/2}$, the second peak is a composite of W^{6+} $4f_{7/2}$ and W^{4+} $4f_{5/2}$, and the third peak belongs to W^{4+} $4f_{7/2}$.

The surface of a film-covered sample was subsequently abraded in a dry inert-gas atmosphere. The process increased the Na(1s) intensity eightfold (80 counts/s) and the O(1s) intensity threefold (630 counts/s) with the intrinsic-to-extrinsic ratio of 5:1. Essentially no change was observed on the W(4f) levels.

The above observations are in accordance with the surface-film formula $Na_xWO_{3-y}(OH)_z$ (see Sec. IV.A). This view was also supported by Auger spectroscopic data (Atoji and Kaminsky, personal communication, 1975). The x value is estimated to be about 0.1-0.3. The x, y, and z values as well as the W^{6+}-W^{4+} distribution vary inhomogeneously on the surface. The abrasion process destroys the film, and the dehydration due to evacuation in the XPS apparatus converts the surface structure to approximately Na_xWO_3 (x = 0.1-0.3).

The chemical-bond irregularities on the surface are balanced out by retaining W^{4+}. The concentration of the oxygen atoms exhibiting the extrinsic-bond character is higher on the surface of the abraded sample.

The film-covered surface was also treated by means of argon-ion sputtering. The sputtering increased the Na(1s) intensity four-to-sevenfold and the O(1s) intensity threefold. The extrinsic O(1s) peak was almost eliminated. The W(4f) photoelectrons enhanced the 33.4-eV peak and produced a new strong peak at 31.2 eV. These results suggest that the sputtering not only destroyed the surface film, but also disrupted some chemical bonds in the substrate. The decomposition species probably include a solid solution composed of Na_xWO_3, W_3O, and metallic tungsten.

The photomicrograph of the argon-sputtered surface is shown in Fig. 22. The surface was originally covered with the birefringent film, which was removed completely by the argon sputtering. There is no direct relation between the domains of the surface film and the pseudodomains produced by the sputtering. In the latter, the domain-wall intersecting angles are 83, 62, 45, and 97°, none of which are interpretable. Moreover, these domains are not birefringent and hence are optically isotropic. The domains are probably an alternating array of two different decomposed species, which were produced by the argon sputtering. This is a remarkable phenomenon and is believed to be the first observation of its kind.

B. Electron Microscopy and Diffraction

Scanning-electron micrographs (SEM's) of several bronze specimens were obtained using the Stereoscan Mark IIA scanning-electron microscope (Cambridge Scientific Instruments, London, England). For details of SEM, see Phillips (1971), Hearle et al. (1972), McCall and Mueller (1973), and Kane and Larrabee (1974). The primary electron voltage was 5 kV, and the mode of operation was secondary-electron emission. Hence, all secondary electrons having an energy of less than 5 kV are participating in forming the image. The emissibility of the secondary electron is roughly proportional to the atomic number of the scatterer in the light atoms up to about Z = 20 (calcium) and then gradually plateaus. However, the surface potential plays a controlling role in the electron emissibility; hence the image brightness in the complex topology is not interpretable straightforwardly. The angle between the direction of the incident beam and the plane of the scatterer was 75° for attaining optimum image contrast, although the 45° setting usually gives the best overall efficiency for collecting secondary electrons.

An epitaxial film that exhibits well-developed twinned domains in the polarized-light microscopy appears untwinned and topologically monotonic in the SEM. Implications of this result are as follows: The film is flat, and hence all domains in the film have the same thickness and no bulging; the emissibility of secondary electrons is nearly isotropic, and hence the anisotropy

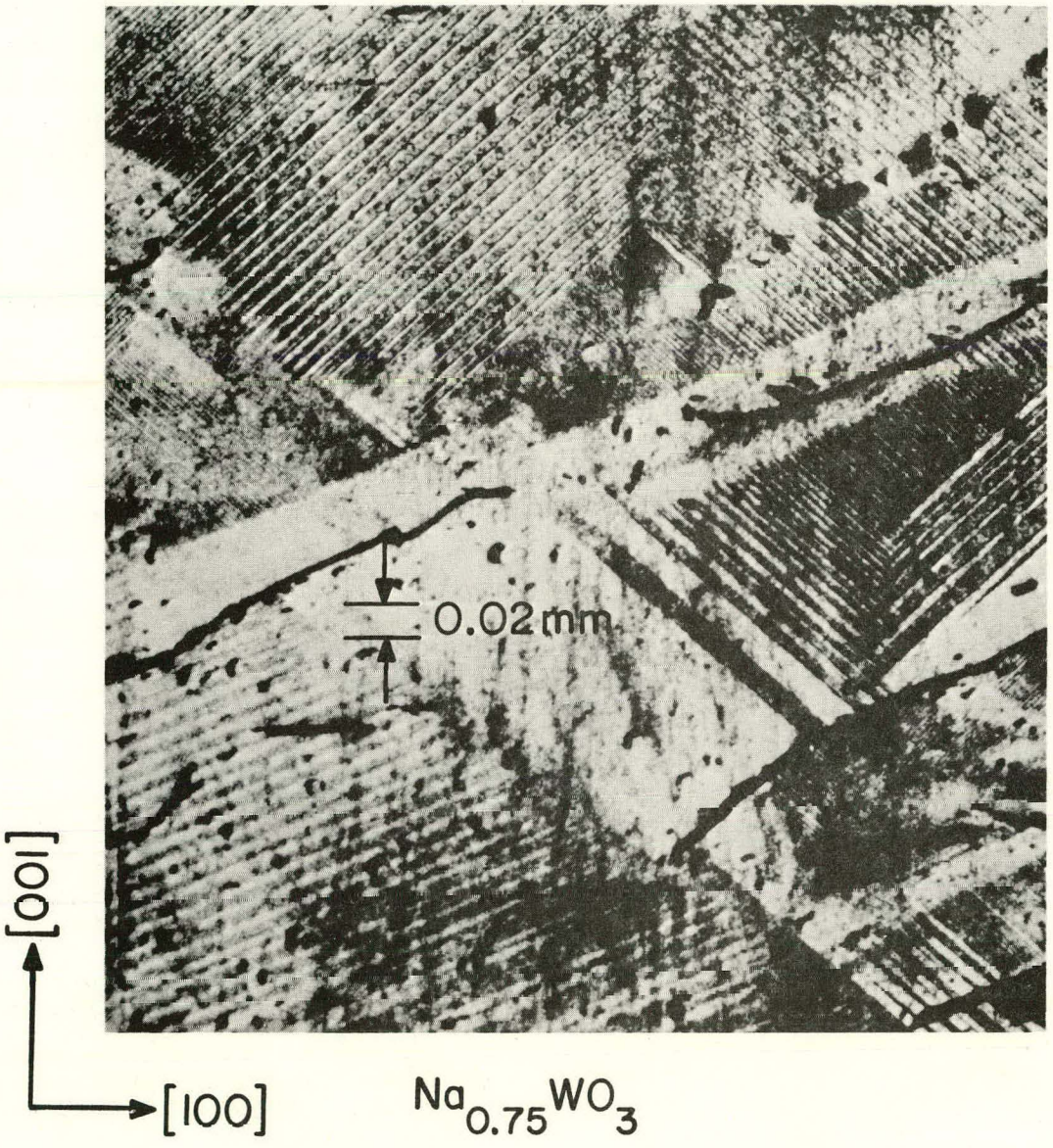

Fig. 22. Unpolarized-light Photomicrograph of Argon-sputtered (010) Surface of $Na_{0.75}WO_3$. ANL Neg. No. 122-78-397.

in the electronic structure is very small. No electron charged-up phenomenon was observed, meaning that the electrons were readily conducted or channeled away.

The etched surface without the epitaxial film shows apex pyramids (see Figs. 23 and 24), which are seen as diamonds in the optical photomicrograph. This apex pyramid is probably a reaction product in the etching (Figs. 8B and 8C) process crystallized epitaxially on the base pyramid.

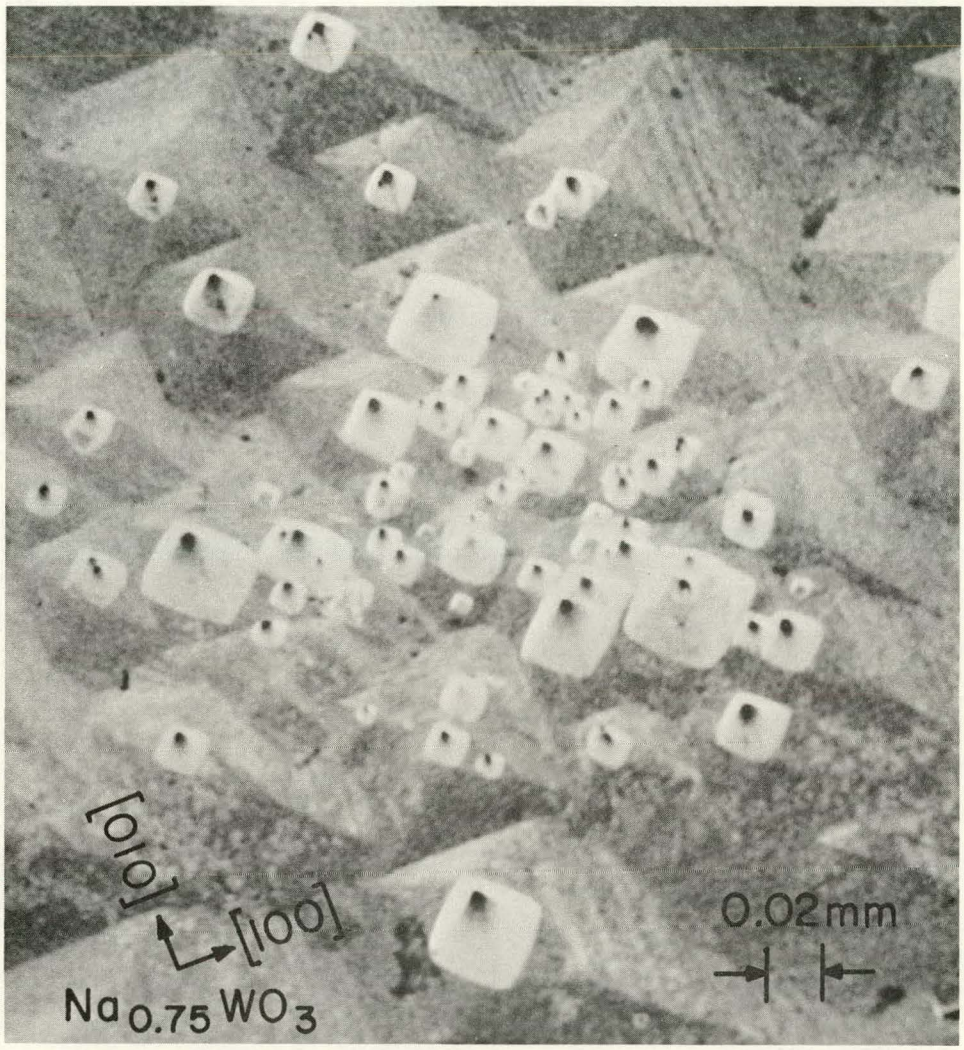

Fig. 23. Scanning-electron Micrograph of Deeply Etched (010) Surface of $Na_{0.75}WO_3$. The bronze specimen was mechanically polished and then etched by a solution of 10% NaOH and 10% $K_3Fe(CN)_6$. The chemical composition of the small, white pyramid on the apex of the base pyramid (cf. Figs. 8B and 8C) should be considerably different from that of other areas. ANL Neg. No. 122-77-928A.

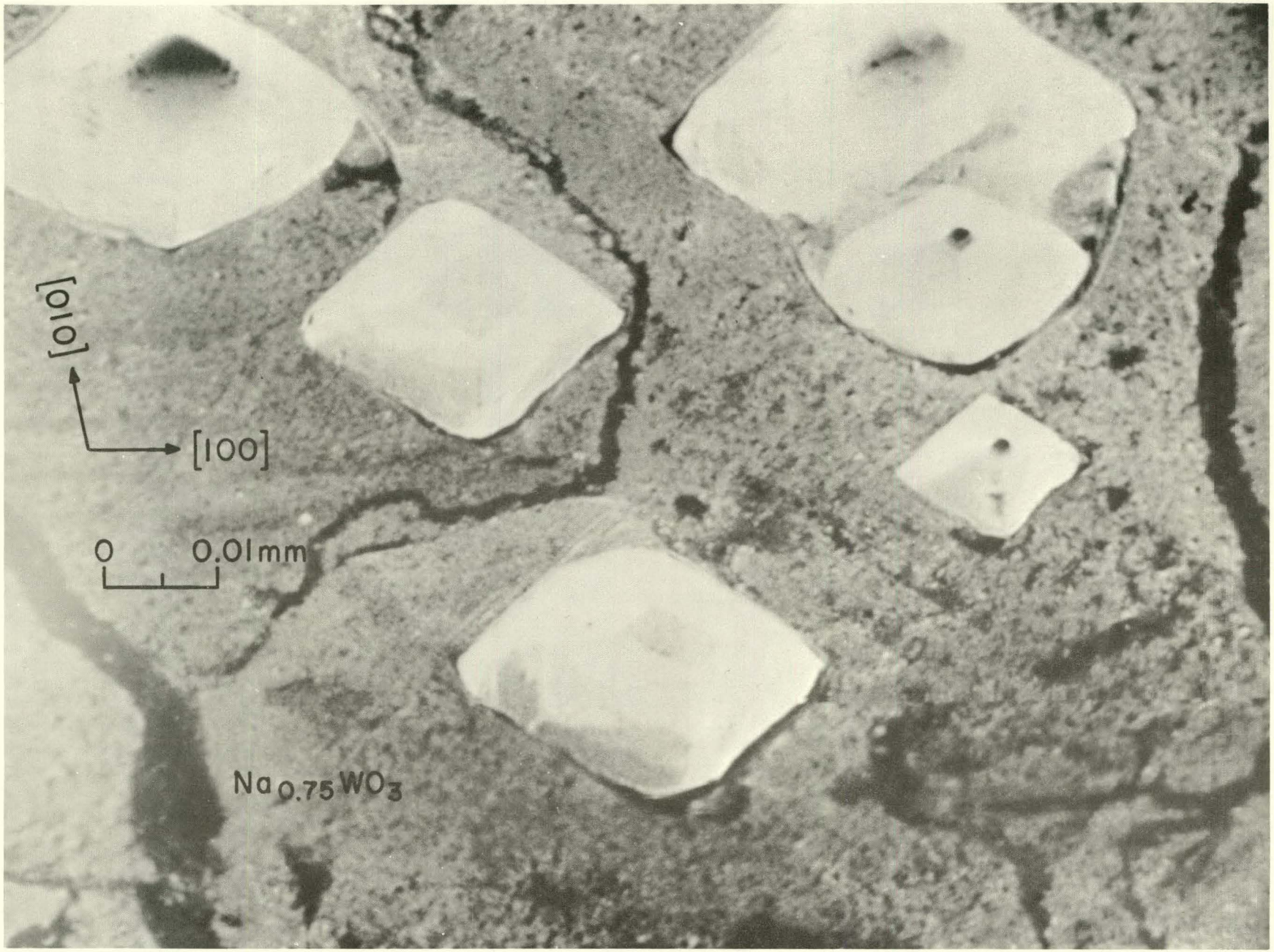

Fig. 24. An Enlarged View of Fig. 23. ANL Neg. No. 122-77-927A.

Preliminary electron-diffraction measurements were performed using 80-kV electron beams of the Siemens 101 Transmission Electron Microscope with a diffraction attachment. The diffraction was made from the thin edge of a small chip obtained by crushing a bronze single crystal in an inert atmosphere. The goniometric device was unavailable, and hence a precision alignment of the crystal was difficult. Nevertheless, some essential aspects of the electron diffraction of the bronze are indicated by the (hh0) and (h 3k k) zones shown in Figs. 25 and 26, respectively. The reflection indices are given in terms of a cubic unit cell containing eight Na_xWO_3 units. In the (hk0) zone, the perovskite structure gives the reflections with h = 2n and k = 2n. However, weak reflections with h = 2n + 1 and k = 2n + 1 were also observed. These extraneous or superlattice reflections are solely attributed to small tilting displacements of the oxygen octahedra from the perovskite structure. Similarly, in (h 3k k), the reflections with k = 2n reflections are attributed to the perovskite structure and those with k = 2n + 1 to the displacement from the perovskite. These superperovskite reflections are too weak to be detectable by X rays but are readily detectable by neutrons (Atoji and Rundle, 1960).

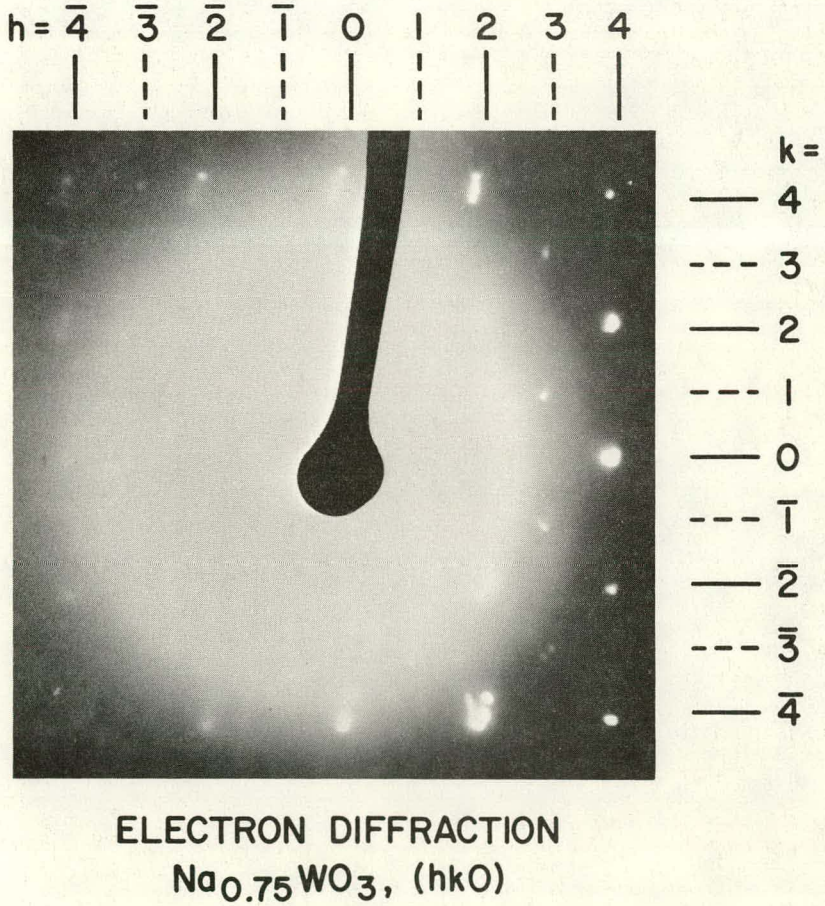

Fig. 25. Electron-diffraction Pattern of (hk0) Zone of $Na_{0.75}WO_3$. The reflections with h = even and k = even are due to the perovskite structure. The reflections with h = odd and k = odd are due to a small deviation from the perovskite structure and are generally very weak. ANL Neg. No. 122-78-695.

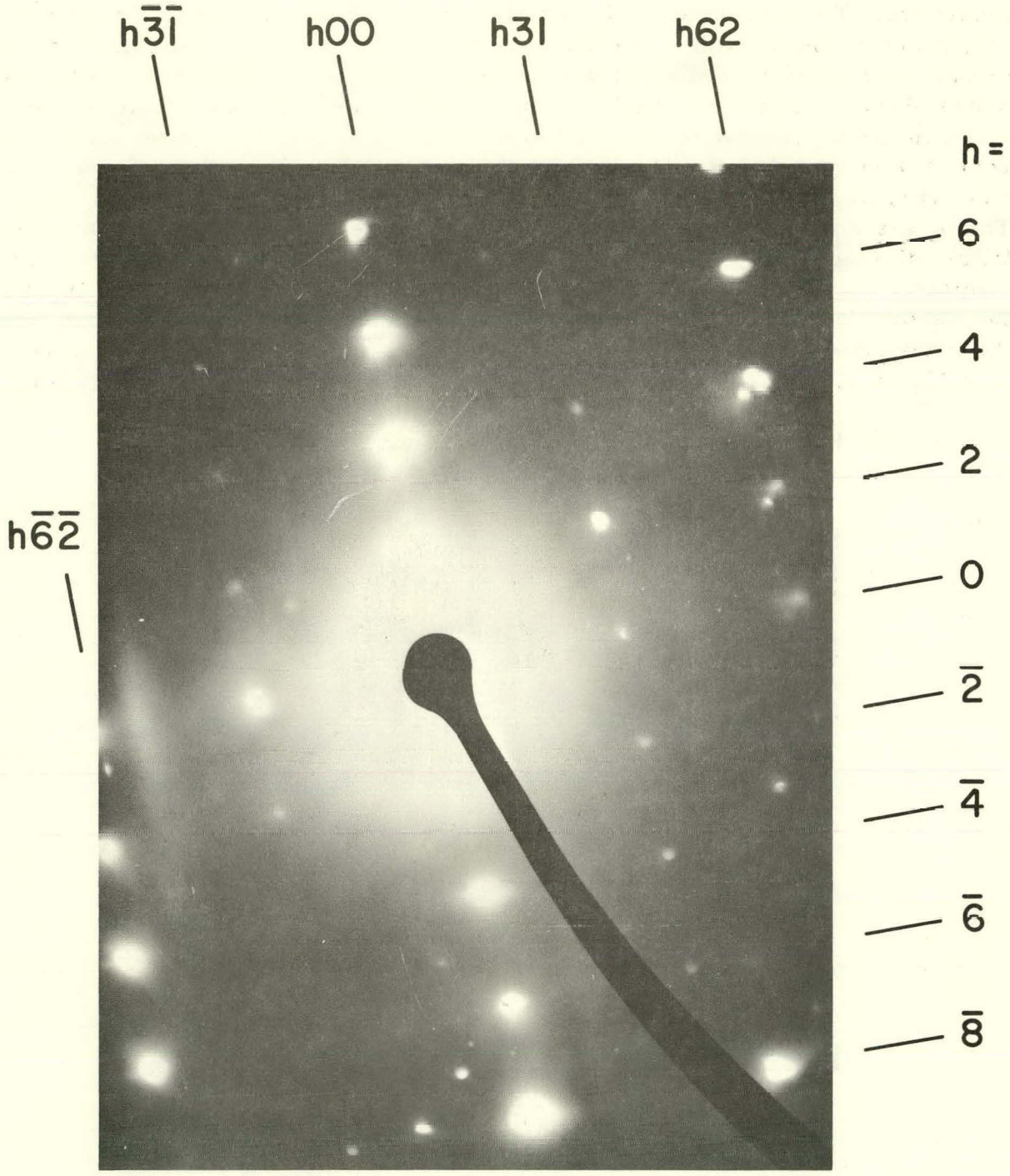

Fig. 26. Electron-diffraction Pattern of (h 3k k) Zone of $Na_{0.75}WO_3$. The reflections with k = even are due to the perovskite structure, and those with k = odd are due to the deviation from the perovskite structure. Some specimen showed strong diffuse streaks on the reciprocal lattice rows of (h00) – (h31) – (h62) – ... . The diffuse streak is strongest in the vicinity of the Bragg reflection. ANL Neg. No. 122-78-696.

ACKNOWLEDGMENTS

I wish to express my sincere appreciation to the following colleagues: G. T. Chubb for the scanning-electron microscopy; G. C. Danielson and R. C. DeVries for supplying bronze specimens used for the early stage of this study; L. H. Fuchs and R. H. Lee for assistance in the metallographic and optical procedures; C. E. Johnson and C. A. Seils for the electron-microprobe analysis; S. A. Johnson for the use of the microscope attachments; M. S. Kaminsky for the Auger spectroscopic analysis; D. W. Lynch for useful information; L. Muldawer for providing unpublished electron-diffraction data; P. R. Okamoto and T. H. Tahmisian for electron-diffraction trials; S. Susman for valuable discussions on optics; and R. J. Thorn for collaborating in the X-ray photoelectron spectroscopy.

REFERENCES

S. Amelinckx and J. Van Landuyt, "The Use of Electron Microscopy in the Study of Extended Defects Related to Non-Stoichiometry," *The Chemistry of Extended Defects in Non-Metallic Solids*, L. Eyring and M. O'Keeffe, Eds., North-Holland Publishing Co., Amsterdam (1970).

M. Amjad and D. Pletcher, *Simple Redox Processes at Tungsten Bronze Electrodes*, J. Electroanal. Chem. Interfacial Electrochem. *59*, 61 (1975).

A. J. Appleby and C. Van Drunen, *Behavior of Pure and Platinum-Doped Sodium Tungsten Bronze Electrodes in Oxygen-Saturated Phosphoric Acid*, J. Electrochem. *123*, 200 (1976).

R. D. Armstrong, A. F. Douglas, and D. E. Williams, *A Study of the Sodium Tungsten Bronzes for Use as Electrocatalysts in Acid Electrolyte Fuel Cells*, Energy Convers. *11*, 7 (1971).

M. Atoji, *Domain Structure of Sodium Tungsten Bronzes, Na_xWO_3 ($0.4 < x < 1$)*, Solid State Commun. *27*, 1227 (1978).

M. Atoji and R. E. Rundle, *Neutron Diffraction Study on Sodium Tungsten Bronzes Na_xWO_3 ($x = 0.9$-0.6)*, J. Chem. Phys. *32*, 627 (1960).

E. Banks, C. W. Fleischmann, and L. Meites, *On the Nature of the Species Reduced During the Electrochemical Synthesis of Tungsten Bronzes*, J. Solid State Chem. *1*, 372 (1970).

D. J. M. Bevan and P. Hagenmuller, *Nonstoichiometric Compounds: Tungsten Bronzes, Vanadium Bronzes, and Related Compounds*, Pergamon Press, New York (1975).

J. O'M. Bockris, A. Damjanovic, and R. J. Mannan, *Catalysis of the Electrodic Hydrogen Evolution and Dissolution Reactions on Rationally Chosen Substrates*, J. Electroanal. Chem. *18*, 349 (1968).

J. O'M. Bockris and J. McHardy, *Electrocatalysis of Oxygen Reduction by Sodium Tungsten Bronze: II. The Influence of Traces of Platinum*, J. Electrochem. Soc. *120*, 61 (1973).

G. Bonera, F. Borsa, M. L. Crippa, and A. Rigamonti, *Transient Nuclear-Magnetic Resonance Study of Phase Transitions in Metallic Sodium Tungsten Bronzes*, Phys. Rev. *B4*, 52 (1971).

E. O. Brimm, J. C. Brantley, J. H. Lorenz, and M. H. Jellinek, *Sodium and Potassium Tungsten Bronzes*, J. Am. Chem. Soc. *73*, 5427 (1951).

B. W. Brown and E. Banks, *The Sodium Tungsten Bronzes*, J. Am. Chem. Soc. *76*, 963 (1954).

B. Broyde, *Tungsten Bronze Fuel Cell Catalysts*, J. Catalysis *10*, 13 (1968).

P. Camagni and A. Manara, *Optical Properties of Metallic Sodium Tungsten Bronzes: Analysis of Free- and Bound-Electron Contributions*, Phys. Rev. *B15*, 4623 (1977a).

P. Camagni and A. Manara, *Electroreflectance vs. Bulk Dielectric Behavior in Metallic Na_xWO_3*, Nuovo Cimento Soc. Ital. Fis. B *39B*, 417 (1977b).

M. Campagna, G. K. Wertheim, H. R. Shanks, F. Zumsteg, and E. Banks, *Local Character of Many-Body Effects in X-Ray Photoemission from Transition-Metal Compounds: Na_xWO_3*, Phys. Rev. Lett. *34*, 738 (1975).

T. A. Carlson, *Photoelectron and Auger Spectroscopy*, Plenum Press, New York (1975).

G. A. Chadwick, *Metallography of Phase Transformations*, Butterworths and Co., London (1972).

J.-N. Chazalviel, M. Campagna, G. K. Wertheim, and H. R. Shanks, *Final-State Effects in the X-Ray Photoelectron Spectra of Cubic Sodium-Tungsten Bronzes*, Phys. Rev. *B16*, 697 (1977).

R. Clarke, *New Sequence of Structural Phase Transitions in Na_xWO_3*, Phys. Rev. Lett. *39*, 1550 (1977).

R. J. Colton and J. W. Rabalais, *Electronic Structure of Tungsten and Some of Its Borides, Carbides, Nitrides, and Oxides by X-Ray Electron Spectroscopy*, Inorg. Chem. *15*, 236 (1976).

F. Consadori and A. Stella, *Optical Reflectivity of Na_xWO_3*, Lett. Nuovo Cimento *3*, 600 (1970).

R. S. Crandall and B. W. Faughnan, *Comment on the Cluster Model of Alkali-Metal Tungsten Bronzes*, Phys. Rev. *B16*, 1750 (1977).

B. A. DeAngelis and M. Schiavello, *The Oxidation State of Tungsten in Na_xWO_3 Bronzes as Determined by X-Ray Photoelectron Spectroscopy*, Chem. Phys. Lett. *38*, 155 (1976).

B. A. DeAngelis and M. Schiavello, *X-Ray Photoelectron Spectroscopy Study of Nonstoichiometric Tungsten Oxides*, J. Solid State Chem. *21*, 67 (1977).

W. F. De Jong, *Die Kristallstrucktur der regulären Na-W-Bronzen*, Z. Kristallogr. *81*, 314 (1932).

R. C. DeMattel, R. A. Huggins, and R. S. Feigelson, *Crystal Growth by the Electrochemical Czochralski Technique (ECT)*, J. Cryst. Growth *34*, 1 (1976).

P. G. Dickens, *Thermodynamic Studies of Some Electrode Materials*, Adv. Chem. Ser. *163*, 165 (1977).

P. G. Dickens, R. M. P. Quilliam, and M. S. Whittingham, *The Reflectance Spectra of the Tungsten Bronzes*, Mater. Res. Bull. *3*, 941 (1968).

P. G. Dickens and M. S. Whittingham, *The Tungsten Bronzes and Related Compounds*, Quart. Rev. Chem. Soc. *22*, 30 (1968).

J. W. Diggle, Ed., *Oxides and Oxide Films*, Marcel Dekker, Inc., New York, Vol. I (1972) and Vol. II (1973).

F. Ebert and H. Flasch, *Röntgenographische Feststellung neuer Verbindungsformen. I. Die Wolframoxyde W_4O_{11} and W_6O_{23}*, Z. Anorg. Allg. Chem. *217*, 95 (1934).

F. Ebert and H. Flasch, *Neue Anschauungen über Niedere Wolframoxyde*, Z. Anorg. Allg. Chem. *226*, 65 (1935).

L. D. Ellerbeck, H. R. Shanks, P. H. Sidles, and G. C. Danielson, *Electrical Resistivity of Cubic Sodium Tungsten Bronze*, J. Chem. Phys. *35*, 298 (1961).

E. Fatuzzo and W. J. Merz, *Ferroelectricity*, Interscience Publishers, New York (1967).

J. H. Fishman, J. F. Henry, and S. Tessore, *Activation of Sodium Tungsten Bronzes with Noble Metals*, Electrochim. Acta *14*, 1314 (1969).

E. J. Flynn, S. A. Solin, and H. R. Shanks, *Raman Active Soft Modes and Phase Transitions in Sodium Tungsten Bronzes,* Solid State Commun. *25,* 743 (1978).

R. A. Fredlein and A. Damjanovic, *Electrochemical Deposition and Dissolution of Tungsten Oxide Bronzes,* J. Solid State Chem. *4,* 94 (1972).

A. T. Fromhold, Jr., and A. Narath, *Transient Nuclear Magnetic Resonance Study of the Conduction Band of Metallic Na_xWO_3: ^{23}Na Relaxation,* Phys. Rev. *136,* A487 (1964).

R. Fuchs, *Electronic Properties of the Tungsten Bronzes,* J. Chem. Phys. *42,* 3781 (1965).

P. Gadó, *X-Ray Powder Diffraction Study of the $WO_3 \rightleftarrows W_{20}O_{58}$ Shear Transformation,* Acta Phys. Acad. Sci. Hung. *18,* 111 (1965).

F. S. Galasso, *Structure, Properties and Preparation of Perovskite-type Compounds,* Pergamon Press, Oxford, England (1969).

F. R. Gamble and T. H. Geballe, "Inclusion Compounds," *Treatise on Solid State Chemistry, Vol. 3, Crystalline and Noncrystalline Solids,* N. B. Hannay, Ed., Chapt. 2, Plenum Press, New York (1976).

W. R. Gardner and G. C. Danielson, *Electrical Resistivity and Hall Coefficient of Sodium Tungsten Bronze,* Phys. Rev. *93,* 46 (1954).

B. C. Gerstein, A. H. Klein, and H. R. Shanks, *Thermal Study of the Tungsten Bronzes: I. Heat Capacity of $Na_{0.679}WO_3$ in the Range 15-300°K,* J. Phys. Chem. Solids *25,* 177 (1964).

R. C. Gifkins, *Optical Microscopy of Metals,* American Elsevier Publishing Co. (1970).

P. Giuliani, A. Gustinetti, and A. Stella, *Optical Transition to the Fermi Level in Na_xWO_3,* Phys. Lett. *38A,* 515 (1972).

A. M. Glazer, *Simple Ways of Determining Perovskite Structures,* Acta Crystallogr. *A31,* 756 (1975).

O. Glemser and C. Naumann, *Kristallisierte Wolframblauverbindungen; Wasserstoffanaloga der Wolframbronzen H_xWO_3,* Z. Anorg. Chem. *265,* 288 (1951).

O. Glemser and H. Sauer, *Uber Wolframoxyde,* Z. Anorg. Allg. Chem. *252,* 156, 159 (1943).

J. B. Goodenough, *Metallic Oxides, Progress in Solid State Chemistry,* H. Reiss, Ed., Pergamon Press, Oxford, Vol. 5, p. 145 (1971).

M. Green, W. C. Smith, and J. A. Weiner, *A Thin Film Electrochromic Display Based on the Tungsten Bronzes,* Thin Solid Films *38,* 89 (1976).

J. D. Greiner, H. R. Shanks, and D. C. Wallace, *Magnetic Susceptibility of the Cubic Sodium Tungsten Bronzes,* J. Chem. Phys. *36,* 772 (1962).

P. Hagenmuller, *Les Bronzes Oxygénés, Progress in Solid State Chemistry,* H. Reiss, Ed., Pergamon Press, Oxford, Vol. 5, p. 71 (1971).

G. Hägg, *Zur Kenntnis der kubischen Natrium-Wolfram-Bronzen,* Z. Phys. Chem. (Leipzig) *B29,* 192 (1935).

G. Hägg and A. Magnéli, *Recent Structure Investigations of Oxygen Compounds of Molybdenum and Tungsten,* Rev. Pure Appl. Chem. (Australia) *4,* 235 (1954).

P. B. Hahn, M. A. Wechter, D. C. Johnson, and A. F. Voigt, *Sodium Tungsten Bronze as a Potentiometric Indicating Electrode for Dissolved Oxygen in Aqueous Solution,* Anal. Chem. *45,* 1016 (1973).

E. O. Hall, *Twinning and Diffusionless Transformations in Metals,* Butterworths Scientific Publications, London (1954).

J. W. S. Hearle, J. T. Sparrow, and P. M. Cross, *The Use of the Scanning Electron Microscope,* Pergamon Press, Oxford (1972).

G. Hoppmann and E. Salje, *Optical and Electrical Properties of H^+ Doped WO_3 Single Crystals,* Phys. Status Solidi (a) *37,* K187 (1976).

A. Hussain and L. Kihlborg, *Intergrowth Tungsten Bronzes,* Acta Crystallogr. *A32,* 551 (1976).

B. G. Hyde and M. O'Keeffe, *Relation Between the $DO_9(ReO_3)$ Structure Type and Some Bronze and Tunnel Structures,* Acta Crystallogr. *A29,* 243 (1973).

H. Inaba and K. Naito, *Specific Heat Measurement of Cubic Sodium Tungsten Bronzes from 200 to 800°K,* J. Solid State Chem. *15,* 283 (1975).

J. H. Ingold and R. C. DeVries, *Twins and Phase Transitions in Sodium Tungsten Bronze,* Acta Metall. *6,* 736 (1958).

F. Jona and G. Shirane, *Ferroelectric Crystals,* Pergamon Press, Oxford (1962).

F. T. Jones, *The Catalytic Activity of Sodium Tungsten Bronzes,* Diss. Abstr. *21,* 1390 (1960).

W. H. Jones, Jr., E. A. Garbaty, and R. G. Barnes, *Nuclear Magnetic Resonance in Metal Tungsten Bronzes,* J. Chem. Phys. *36,* 494 (1962).

W. A. Kamitakahara, B. N. Harmon, J. G. Taylor, L. Kopp, and H. R. Shanks, *Concentration-Dependent Kohn Effect in Cubic Tungsten Bronzes,* Phys. Rev. Lett. *36,* 1393 (1976).

P. F. Kane and G. B. Larrabee, Eds., *Characterization of Solid Surfaces,* Plenum Press, New York (1974).

H. F. Kay, *Preparation and Properties of Crystals of Barium Titanate, $BaTiO_3$,* Acta Crystallogr. *1,* 229 (1948).

G. K. Kehl, *The Principles of Metallographic Laboratory Practice,* 3rd Ed., McGraw-Hill, New York (1949).

J. M. Keller, *Conduction Electrons in Sodium Tungsten Bronze,* J. Chem. Phys. *33,* 232 (1960).

M. V. Klassen-Neklyudova, translated by J. E. S. Bradley, *Mechanical Twinning of Crystals,* Consultants Bureau, New York (1964).

B. Kopelman, *Tungsten Bronze Rectifiers,* U. S. Patent, 2,760,126 (Aug 21, 1956).

L. Kopp, B. N. Harmon, and S. H. Liu, *Band Structure of Cubic Na_xWO_3,* Solid State Commun. *22,* 677 (1977).

F. Kupka and M. J. Sienko, *The Magnetic Susceptibility of Tungsten Bronzes,* J. Chem. Phys. *18,* 1296 (1950).

M. A. Langell and S. L. Bernasek, *Leed/Auger Observations of Cubic Sodium Tungsten Bronze Single Crystals,* Surf. Sci. *69,* 727 (1977).

P. A. Lightsey, *Percolation View of Transport Properties in Na_xWO_3,* Phys. Rev. *B8,* 3586 (1973).

P. A. Lightsey, D. A. Lilienfeld, and D. F. Holcomb, *Transport Properties of Cubic Na_xWO_3 Near the Insulator-Metal Transition,* Phys. Rev. *B14,* 4730 (1976).

B. O. Loopstra and P. Boldrini, *Neutron Diffraction Investigation of WO_3,* Acta Crystallogr. *21,* 158 (1966).

D. W. Lynch, R. Rosei, J. H. Weaver, and C. G. Olson, *The Optical Properties of Some Alkali Metal Tungsten Bronzes from 0.1 to 38 eV,* J. Solid State Chem. *8,* 242 (1973).

A. R. Mackintosh, *Model for the Electronic Structure of Metal Tungsten Bronzes,* J. Chem. Phys. *38,* 1991 (1963).

A. Magnéli, *Notes on the Analysis of Tungsten Bronzes,* Ark. Kemi *1,* 273 (1949a).

A. Magnéli, *Crystal Structure Studies on Tetragonal Sodium Tungsten Bronze,* Ark. Kemi *1,* 269 (1949b).

J. L. McCall and W. M. Mueller, Ed., *Metallographic Specimen Preparation, Optical and Electron Microscopy,* Plenum Press, New York (1973).

G. E. McGuire and T. A. Carlson, *Study of the X-Ray Photoelectron Spectrum of Tungsten-Tungsten Oxide as a Function of Thickness of the Surface Oxide Layer,* J. Electron Spectrosc. *1,* 161 (1972/1973).

J. McHardy and J. O'M. Bockris, *Electrocatalysis of Oxygen Reduction by Sodium Tungsten Bronze I. Surface Characteristics of a Bronze Electrode,* J. Electrochem. Soc. *120,* 53 (1973).

R. S. Mitchell, *X-Ray Data for Hydrotungstite,* Am. Mineral. *48,* 935 (1963).

T. Mitsui and J. Furuichi, *Domain Structure of Rochelle Salt and KH_2PO_4,* Phys. Rev. *90,* 193 (1953).

S. S. Moody and D. Taylor, *Catalytic Decomposition of Formic Acid on Sodium Tungsten Bronzes,* J. Chem. Soc. Faraday Trans. *73,* 289 (1973).

L. D. Muhlestein and G. C. Danielson, *Seebeck Effect in Sodium Tungsten Bronze,* Phys. Rev. *160,* 562 (1967a).

L. D. Muhlestein and G. C. Danielson, *Effects of Ordering on the Transport Properties of Sodium Tungsten Bronze,* Phys. Rev. *158,* 825 (1967b).

L. Muldawer, *Electron Diffraction in Surfaces of Sodium Tungsten Bronzes,* Department of Physics, Temple University (1962).

T. Nakamura, *On the Domain Structure of Rochelle Salt Crystal,* J. Phys. Soc. Japan *11,* 624 (1956a).

T. Nakamura, *On the Correlation Between Screw Dislocations and Twin Structure in WO_3 Crystal,* J. Phys. Soc. Japan *11,* 467 (1956b).

K. L. Ngai and R. Silberglitt, *Effect of Lattice Instability on Superconductivity in Sodium Tungsten Bronze,* Phys. Rev. *B13,* 1032 (1976).

L. W. Niedrach and H. I. Zeliger, *Catalytic Enhancement of Carbon Monoxide and Reformer Gas Oxidation in Fuel Cells by Sodium Tungsten Bronzes,* J. Electrochem. Soc. *116,* 152 (1969).

Jul. Philipp and P. Schwebel, *Zur Kenntniss der Wolframbronce,* Ber. *12,* 2234 (1879).

V. A. Phillips, *Modern Metallographic Techniques and Their Applications,* Wiley-Interscience, New York (1971).

E. Polaczkowa and A. Polaczek, *Cubic Tungsten Bronzes of Sodium and Rare Earth Metals. Structural Problems and Magnetic Properties,* Pr. Kom. Ceram., Ceram. Pol. Akad. Nauk. *21,* 29 (1974).

T. A. Ramanarayanan and W. L. Worrell, *A Thermodynamic Investigation of Cubic Sodium Tungsten Bronze, Na_xWO_3,* J. Electrochem. Soc. *121,* 1530 (1974).

J.-P. Randin, *Kinetics of Anodic Oxide Growth on Sodium Tungsten Bronzes,* J. Electrochem. Soc. *120,* 378 (1973).

J.-P. Randin, *Alternating Current Impedance Characteristics of Reduced and Oxidized Sodium-Tungsten Bronze Electrodes,* Electrochim. Acta *19,* 87 (1974a).

J.-P. Randin, *Kinetics of the Electrochemical Deposition and Dissolution of Sodium Tungsten Bronzes,* Electrochim. Acta *19,* 745 (1974b).

J.-P. Randin, *Inhibition Effects in the Electrochemical Reduction of Hydrogen Peroxide on Sodium Tungsten Bronzes,* Can. J. Chem. *52,* 2542 (1974c).

J.-P. Randin, *The Electroreduction of Oxygen and Hydrogen Perioxide of Sodium Tungsten Bronzes,* J. Electrochem. Soc. *121,* 1029 (1974d).

J.-P. Randin, *The Electroreduction of Oxygen and Hydrogen Peroxide of Sodium Tungsten Bronzes: Discussion,* J. Electrochem. Soc. *122,* 742 (1975).

J.-P. Randin and A. K. Vijh, *Hydrogen Evolution Reaction on Sodium Tungsten Bronzes,* Electrochim. Acta *20,* 37 (1975).

J.-P. Randin, A. K. Vijh, and A. B. Chughtai, *Electrochemical Behavior of Sodium Tungsten Bronze Electrodes in Acid Media,* J. Electrochem. Soc. *120,* 1174 (1973).

R. E. Reed-Hill, J. P. Hirth, and H. C. Rogers, Eds., "Deformation Twinning," *Metallurgical Society Conferences,* Vol. 25, American Institute of Mining, Metallurgical and Petroleum Engineers, Inc., Gordon and Breach Science Publishers, New York (1964).

C. N. Reid, *A Review of Mechanical Twinning in Body-Centered Cubic Metals and Its Relation to Brittle Fracture,* J. Less-Common Metals *9,* 105 (1965).

A. S. Ribnick, B. Post, and E. Banks, *Phase Transitions in Sodium Tungsten Bronzes. Nonstoichiometric Compounds,* Adv. Chem. Ser. *39,* 246 (1963).

G. D. Rieck, *Tungsten and Its Compounds,* Pergamon Press, Oxford (1967).

J. G. Roper and H. B. Knowles, *Sodium Ordering in Sodium Tungsten Bronzes,* Phys. Lett. *38A,* 477 (1972).

C. Rosen, E. Banks, and B. Post, *The Thermal Expansion and Phase Transitions of WO_3,* Acta Crystallogr. *9,* 475 (1956a).

C. Rosen, B. Post, and E. Banks, *The Thermal Expansion of Cubic Sodium Tungsten Bronzes,* Acta Crystallogr. *9,* 477 (1956b).

L. E. Samuels, *Metallographic Polishing by Mechanical Methods,* 2nd Ed., Sir Isaac Pitman and Sons, Ltd., Melbourne (1971).

S. Sawada, *Thermal and Electrical Properties of Tungsten Oxide (WO_3),* J. Phys. Soc. Japan *11,* 1237 (1956a).

S. Sawada, *Microscopic and X-Ray Studies on Tungsten Oxide (WO_3),* J. Phys. Soc. Japan *11,* 1246 (1956b).

S. Sawada and G. C. Danielson, *Electrical Conduction in Crystals and Ceramics of WO_3,* Phys. Rev. *113,* 803 (1959a).

S. Sawada and G. C. Danielson, *Domain Structure of WO_3 Single Crystals,* Phys. Rev. *113,* 1005 (1959b).

S. Sawada and G. C. Danielson, *Optical Indices of Refraction of WO_3,* Phys. Rev. *113,* 1008 (1959c).

J. F. Scott and R. F. Leheny, *Raman Study of Metallic Tungsten Bronzes,* Phys. Rev. *B2,* 3883 (1970).

D. B. Šepa, A. Damjanovic, and J. O'M. Bockris, *Sodium Tungsten Bronzes as Electrodes for Oxygen Reduction,* Electrochim. Acta *12,* 746 (1967).

D. B. Šepa, D. S. Ovcin, and M. V. Vojnović, *Hydrogen Evolution Reaction at Sodium Tungsten Bronzes in Acid Solutions,* J. Electrochem. Soc. *119,* 1285 (1972).

D. B. Šepa, M. V. Vojnović, D. S. Ovcin, and N. D. Pavlović, *Behavior of Sodium Tungsten Bronze Electrode in Alkaline Solutions,* Electroanal. Chem. Interfacial Electrochem. *51,* 99 (1974).

H. R. Shanks, *Growth of Tungsten Bronze Crystals by Fused Salt Electrolysis,* J. Cryst. Growth *13/14,* 433 (1972).

H. R. Shanks, *Enhancement of the Superconducting Transition Temperature Near a Phase Instability in Na_xWO_3,* Solid State Commun. *15,* 753 (1974).

H. R. Shanks and R. D. Redin, *The Thermal Conductivity of Some Sodium Tungsten Bronzes,* J. Phys. Chem. Solids *27,* 75 (1966).

H. R. Shanks, P. H. Sidles, and G. C. Danielson, *Electrical Properties of the Tungsten Bronzes: Nonstoichiometric Compounds,* Adv. Chem. Ser. *39,* 237 (1963).

M. J. Sienko, *Electrical and Magnetic Properties of the Tungsten and Vanadium Bronzes: Nonstoichiometric Compounds,* Adv. Chem. Ser. *39,* 224 (1963).

J. S. Smith, *Electrostatic Energy Calculations for Sodium Tungsten Bronzes (Na_xWO_3),* Phys. Rev. *95,* 1369 (1954).

J. F. Smith and G. C. Danielson, *Sodium Diffusion in Sodium Tungsten Bronze,* J. Chem. Phys. *22,* 266 (1954).

V. Spitzin and L. Kaschtanoff, *Bieträge zur analytischen Chemie des Wolframs. II. Quantitative Analyse von Wolframverbindungen auf trockenem Wege,* Z. Anal. Chem. *75,* 440 (1928).

J. Spyridelis, P. Delavignette, and A. Amelinckx, *Non-stoichiometry and Interfacial Dislocations in Tungsten Trioxide,* Mater. Res. Bull. *2,* 615 (1967).

M. E. Straumanis, *The Sodium Tungsten Bronzes. I. Chemical Properties and Structure,* J. Am. Chem. Soc. *71,* 679 (1949).

M. E. Straumanis and A. Dravnieks, *The Sodium Tungsten Bronzes. II. The Electrical Conductivity of the Bronzes,* J. Am. Chem. Soc. *71,* 683 (1949).

T. Takamori and M. Tomozawa, *Thermal Expansion of a Cubic Sodium Tungsten Bronze,* J. Am. Ceram. Soc. *47,* 472 (1964).

F. Takusagawa and R. A. Jacobson, *Crystal Structure Studies of Tetragonal Sodium Tungsten Bronzes, Na_xWO_3. I. $Na_{0.33}WO_3$ and $Na_{0.48}WO_3$,* J. Solid State Chem. *18,* 163 (1976).

S. Tanisaki, *Phase Transition in Tungsten Trioxide,* J. Phys. Soc. Japan *14,* 680 (1959a).

S. Tanisaki, *Observation of a Peculiar Type of Domain Structure of Triclinic Tungsten Trioxide,* J. Phys. Soc. Japan *14,* 970 (1959b).

G. H. Taylor, *Domain Structure in Sodium Tungsten Bronzes,* J. Solid State Chem. *1,* 359 (1969).

B. E. Taylor and P. F. Weller, *Thermal and Electrical Properties of Sodium Tungsten Bronze,* J. Solid State Chem. *1,* 210 (1970).

W. J. McG. Tegart, *The Electrolytic and Chemical Polishing of Metals,* 2nd Ed., Pergamon Press, London (1959).

D. P. Tunstall, *Nuclear-resonance Investigation of the Low-Mobility Region in Cubic Metallic Sodium Tungsten Bronze, Na_xWO_3,* Phys. Rev. *B11,* 2821 (1975).

D. P. Tunstall, *Microscopic Inhomogeneity in Sodium Tungsten Bronze: A Comment,* Phys. Rev. *B14,* 4735 (1976).

R. Ueda and T. Ichinokawa, *Effect of Stress on Domain Structure of Tungsten Trioxide WO_3,* J. Phys. Soc. Japan *6,* 122 (1951).

R. W. Vest, M. Griffel, and J. F. Smith, *Heat Capacity of Sodium Tungsten Bronzes from 1.8 to 4.2°K,* J. Chem. Phys. *28,* 293 (1958).

D. van Duyn, *Contribution à la Connaissance des Bronzes de Tungstène,* Recl. Trav. Chim. Pays-Bas Belg. *61,* 669 (1942).

M. V. Vojnović and D. B. Šepa, *Effect of Electrode Materials on the Kinetics of Electron Exchange Reactions,* J. Chem. Phys. *51,* 5344 (1969).

M. V. Vojnović, D. B. Šepa, and D. S. Ovcin, *The Surface of Sodium Tungsten Bronze Electrodes in Acid Solutions,* Croat. Chem. Acta *44,* 89 (1972).

J. Vondrak and J. Balej, *Electrochemical Properties of Tungsten Bronzes: I. Hydrogen Absorption in Sodium Tungsten Bronzes,* Electrochim. Acta *18,* 1017 (1973).

J. Vondrak and J. Balej, *Electrochemical Properties of Tungsten Bronzes: II. Hydrogen Evolution on Sodium Tungsten Bronzes,* Electrochim. Acta *20,* 283 (1975).

A. D. Wadsley, "Inorganic Non-Stoichiometric Compounds," *Non-Stoichiometric Compounds,* L. Mandelcorn, Ed., Academic Press, New York, Chapter 3 (1964).

M. F. Weber and H. R. Shanks, *Surface and Electrocatalytic Properties of Tungsten Bronzes,* National Bureau of Standards Special Publication 455 (1976).

I. Webman, J. Jortner, and M. H. Cohen, *Electronic Transport in Alkali-Tungsten Bronzes,* Phys. Rev. *B13,* 713 (1976).

M. A. Wechter, H. R. Shanks, G. Carter, G. M. Ebert, R. Guglielmino, and A. F. Voigt, *Use of Metal Tungsten Bronze Electrodes in Chemical Analysis,* Anal. Chem. *44,* 850 (1972).

M. A. Wechter, H. R. Shanks, and A. F. Voigt, *Relations Between Lattice Parameter and x Value for Some Cubic Tungsten Bronzes,* Inorg. Chem. *7,* 845 (1968).

M. A. Wechter, P. B. Hahn, G. M. Ebert, P. R. Montoya, and A. F. Voigt, *Chelometric Titrations of Metal Cations Using the Tungsten Bronze Electrode,* Anal. Chem. *46,* 1267 (1973).

B. R. Weinberger, *Nuclear-Magnetic-Resonance Study of the Cubic Alkali Tungsten Bronzes,* Phys. Rev. *B17,* 566 (1978).

P. F. Weller and D. M. Grandits, *Kyropoulos Single Crystal Growth of Sodium Tungsten Bronzes,* J. Cryst. Growth *12,* 63 (1972).

G. K. Wertheim, M. Campagna, J.-N. Chazalviel, and H. R. Shanks, *Oxidation States of Tungsten in the Na_xWO_3 Bronzes,* Chem. Phys. Lett. *44,* 50 (1976).

M. S. Whittingham, *Free Energy of Formation of Sodium Tungsten Bronzes, Na_xWO_3,* J. Electrochem. Soc. *122,* 714 (1975).

M. S. Whittingham and R. A. Huggins, "Electrochemical Preparation and Characterization of Alkali Metal Tungsten Bronzes, M_xWO_3," National Bureau of Standards Special Publication 364, Solid State Chemistry, *Proc. 5th Materials Research Symposium* (July 1972).

P. J. Wiseman and P. G. Dickens, *The Crystal Structure of Cubic Hydrogen Tungsten Bronze,* J. Solid State Chem. *6,* 374 (1973).

P. J. Wiseman and P. G. Dickens, *Neutron Diffraction Studies of Cubic Tungsten Bronzes,* J. Solid State Chem. *17,* 91 (1976).

F. Wöhler, *Uber das Wolfram,* Ann. Phys. *2,* 350 (1824).

F. C. Zumsteg, *Heat Capacity and Magnetic Susceptibility of Na_xWO_3,* Phys. Rev. *B14,* 1406 (1976).

Distribution for ANL-78-63

Internal:

M. V. Nevitt
B. Ancker-Johnson
P. R. Fields
B. R. T. Frost
G. T. Garvey
D. C. Price
M. Atoji (81)
A. B. Krisciunas
ANL Contract File
ANL Libraries (5)
TIS Files (6)

External:

DOE-TIC, for distribution per UC-4 (181)
Manager, Chicago Operations Office
Chief, Office of Patent Counsel, CH
President, Argonne Universities Association
Chemistry Division Review Committee:
- J. Bigeleisen, SUNY at Stony Brook
- F. A. Cotton, Texas A&M U.
- H. F. Franzen, Iowa State U.
- H. S. Gutowsky, U. Illinois
- D. R. Herschbach, Harvard U.
- E. L. Muetterties, Cornell U.
- F. S. Rowland, U. California, Irvine
- T. T. Sugihara, Texas A&M U.
- J. H. Wang, SUNY at Buffalo